Published on MNRAS, https://doi.org/10.1093/mnras/stae2048

The cosmic rate of Pair-Instability Supernovae

Francesco Gabrielli, Andrea Lapi, Lumen Boco, Cristiano Ugolini, Guglielmo Costa, Cecilia Sgalletta, Kendall Shepherd, Ugo Niccolò Di Carlo, Alessandro Bressan, Marco Limongi, Mario Spera

INFN Istituto Nazionale di Fisica Nucleare

INAF Istituto Nazionale di Astrofisica

SISSA

CRAL Centre de Recherche Astrophysique de Lyon

KAVLI IPMU

Francesco Gabrielli, 4th-year PhD student

An extraordinary journey into the transient sky, Padova, 03/04/2025

very-massive stars

low metallicity

$Z < Z_\odot/2$ Langer et al. 2007

$Z < Z_\odot/3$ Higgins et al. 2021

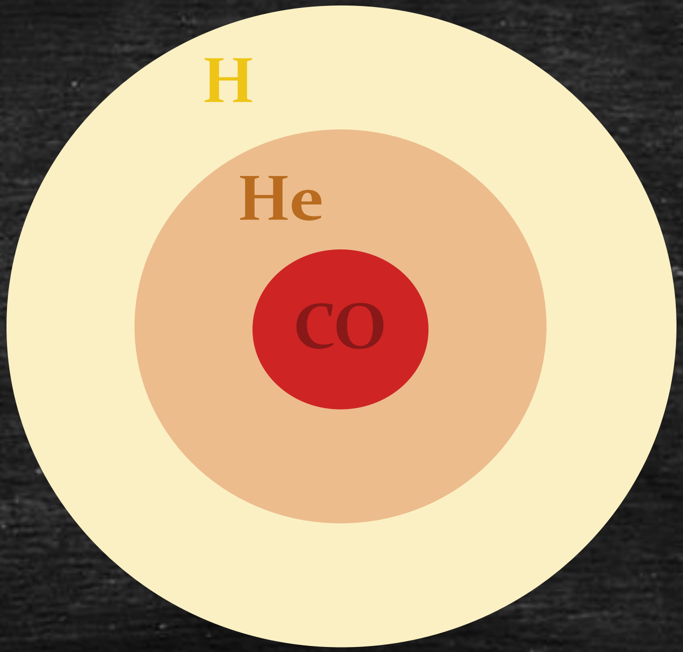

$100\ M_\odot$ | $140\ M_\odot$ | $260\ M_\odot$ | $300\ M_\odot$

Heger & Woosley 2002
Heger et al. 2003

very-massive stars

low metallicity

$Z < Z_\odot/2$ Langer et al. 2007

$Z < Z_\odot/3$ Higgins et al. 2021

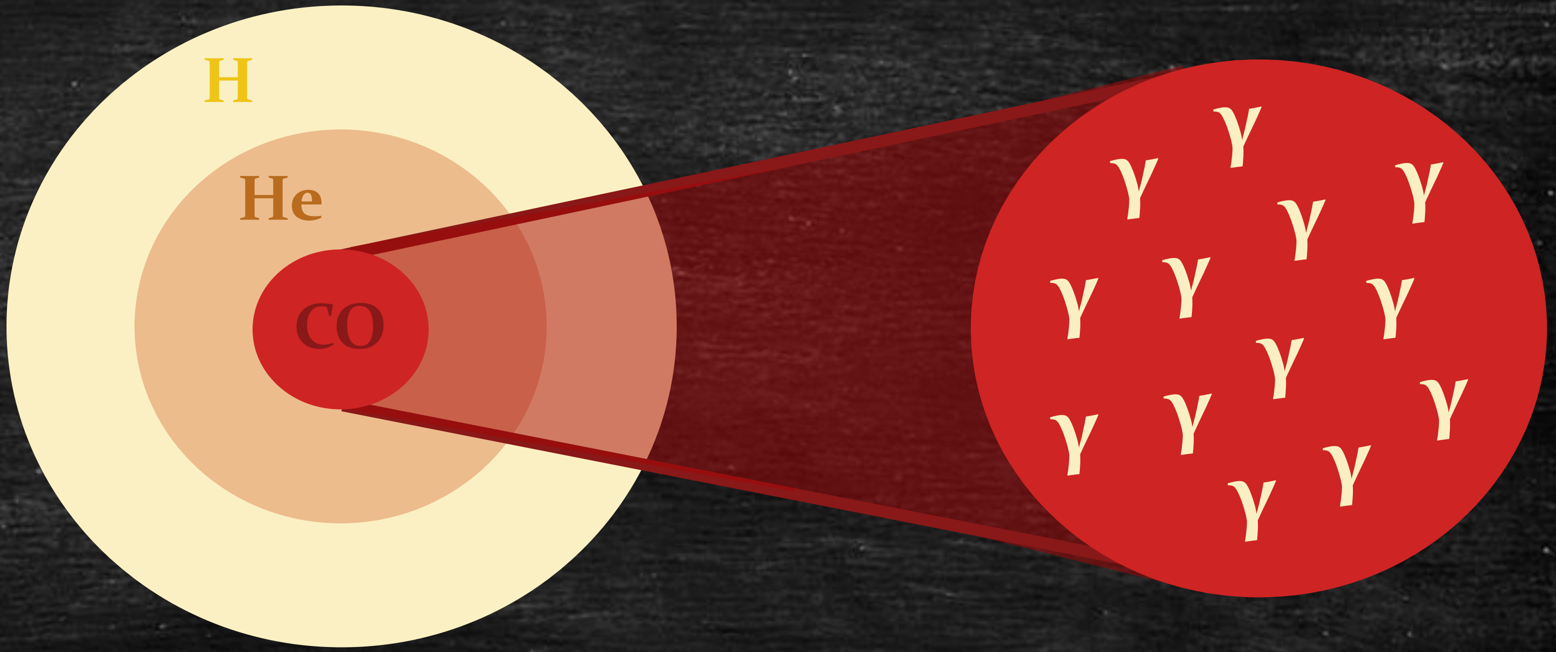

$100\ M_\odot$ | $140\ M_\odot$ | $260\ M_\odot$ | $300\ M_\odot$

Heger & Woosley 2002
Heger et al. 2003

very-massive stars

low metallicity

$Z < Z_\odot/2$ Langer et al. 2007

$Z < Z_\odot/3$ Higgins et al. 2021

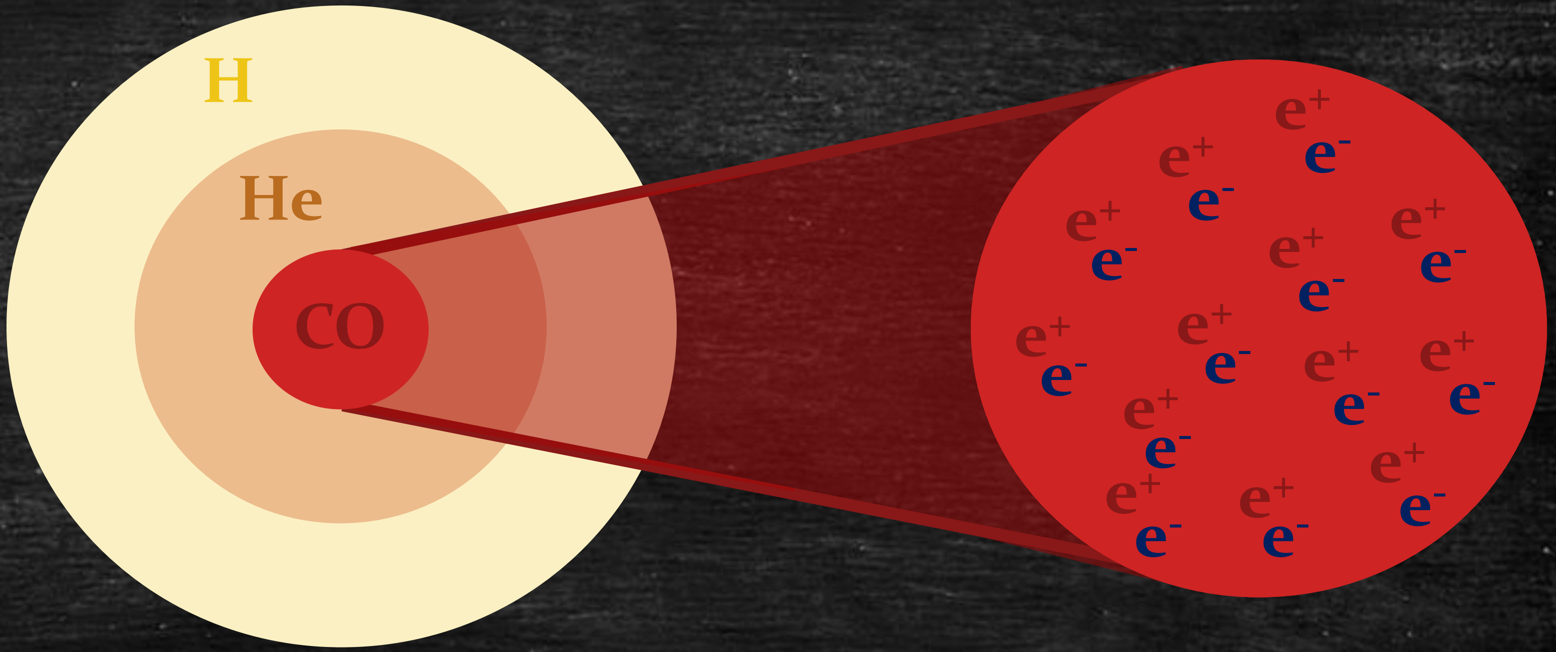

$100\ M_\odot$

$140\ M_\odot$

Heger & Woosley 2002
Heger et al. 2003

$260\ M_\odot$

$300\ M_\odot$

very-massive stars

low metallicity

$Z < Z_\odot/2$ Langer et al. 2007

$Z < Z_\odot/3$ Higgins et al. 2021

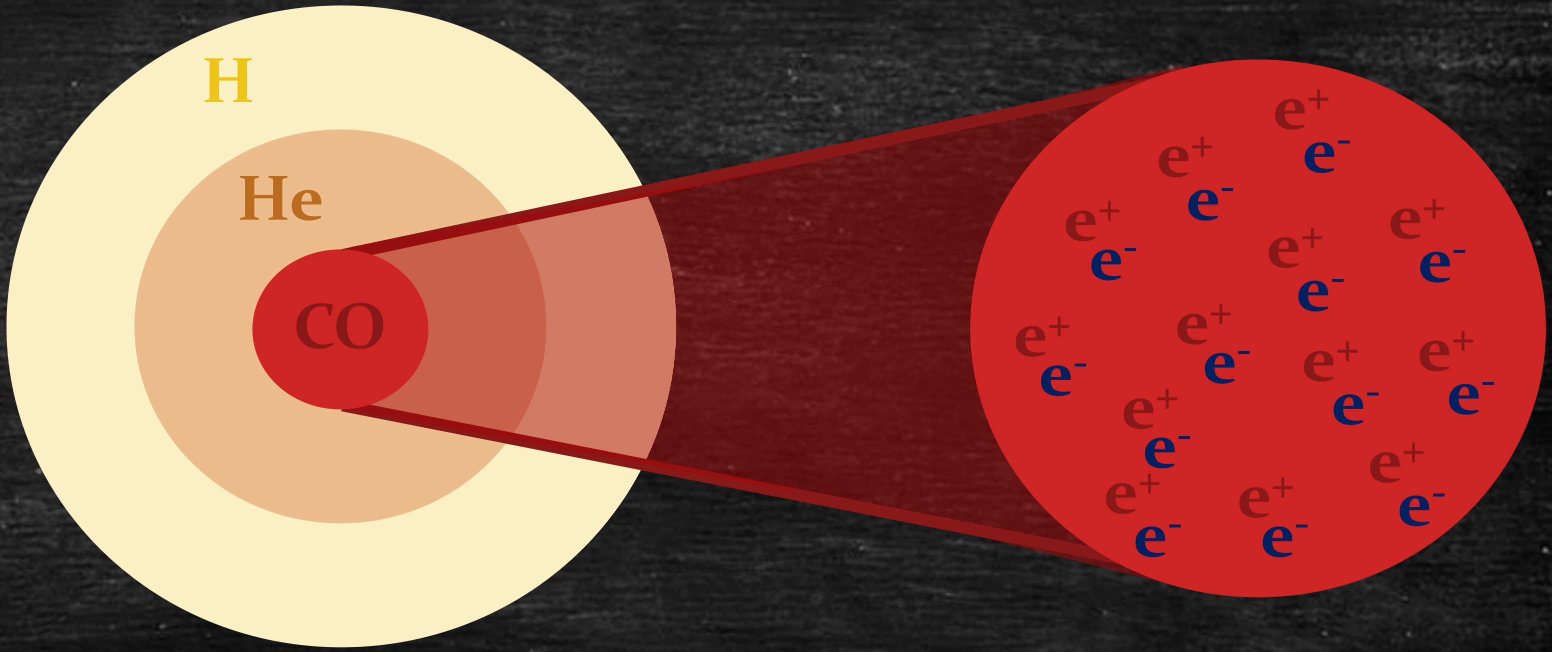

PPISN

$100\ M_\odot$

$140\ M_\odot$

Heger & Woosley 2002
Heger et al. 2003

$260\ M_\odot$

$300\ M_\odot$

very-massive stars

low metallicity

$Z < Z_{\odot}/2$ Langer et al. 2007

$Z < Z_{\odot}/3$ Higgins et al. 2021

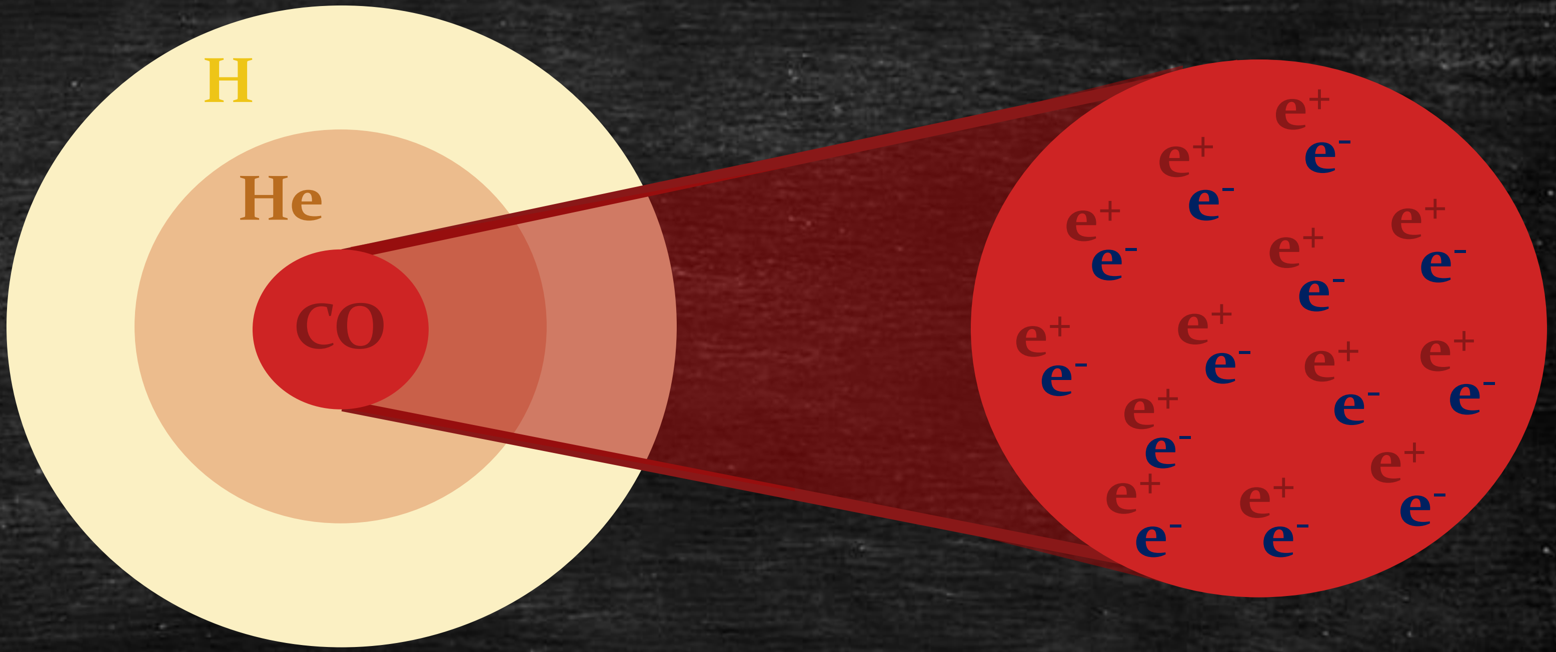

PPISN | **PISN**

$100\ M_{\odot}$ | $140\ M_{\odot}$ | $260\ M_{\odot}$ | $300\ M_{\odot}$

Heger & Woosley 2002
Heger et al. 2003

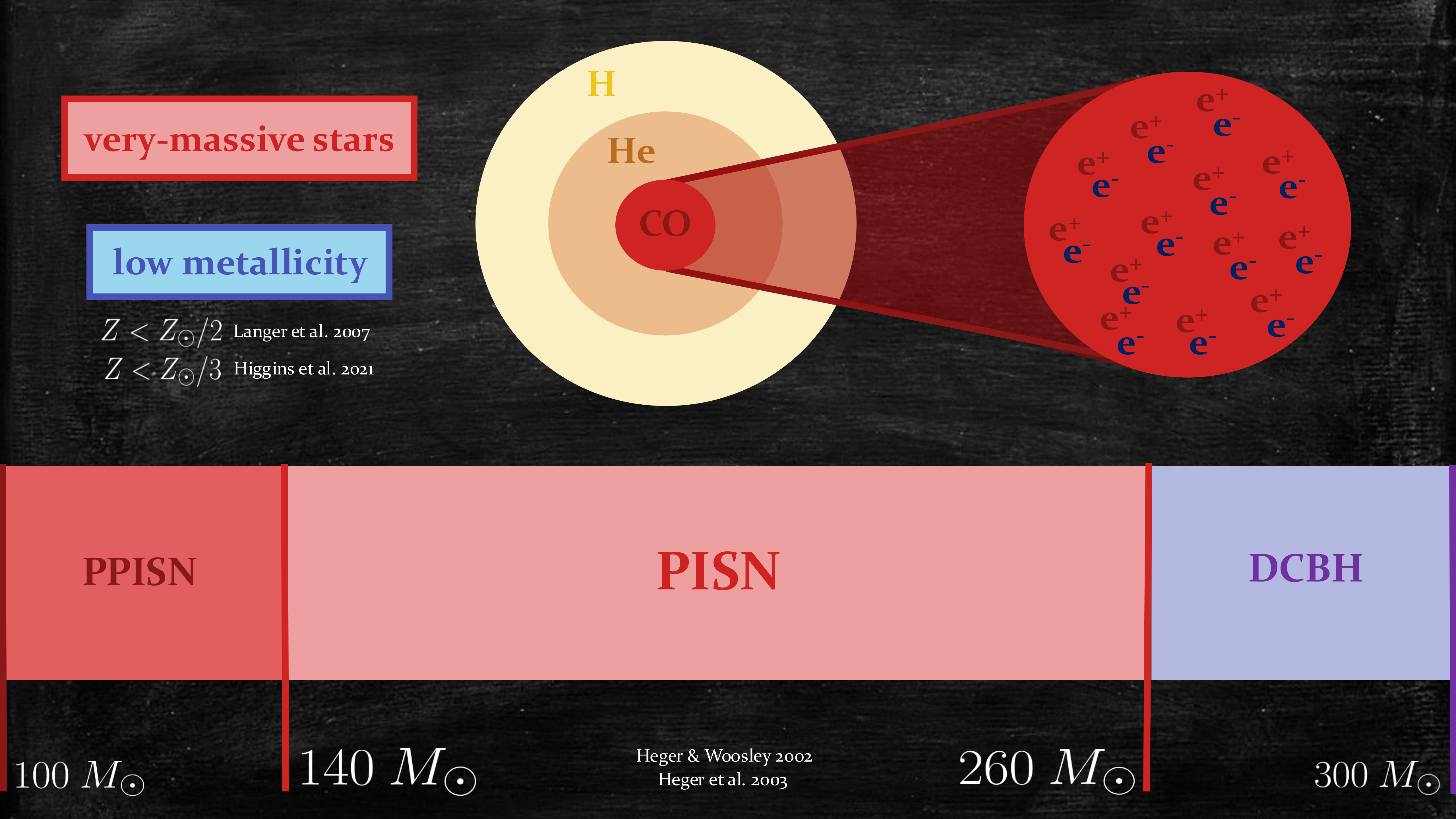
very-massive stars
low metallicity
$Z < Z_\odot/2$ Langer et al. 2007
$Z < Z_\odot/3$ Higgins et al. 2021
H
He
CO
e^+
e^-
PPISN
PISN
DCBH
$100\ M_\odot$
$140\ M_\odot$
Heger & Woosley 2002
Heger et al. 2003
$260\ M_\odot$
$300\ M_\odot$

very-massive

low metalli

$Z < Z_\odot/2$ Langer e

$Z < Z_\odot/3$ Higgins

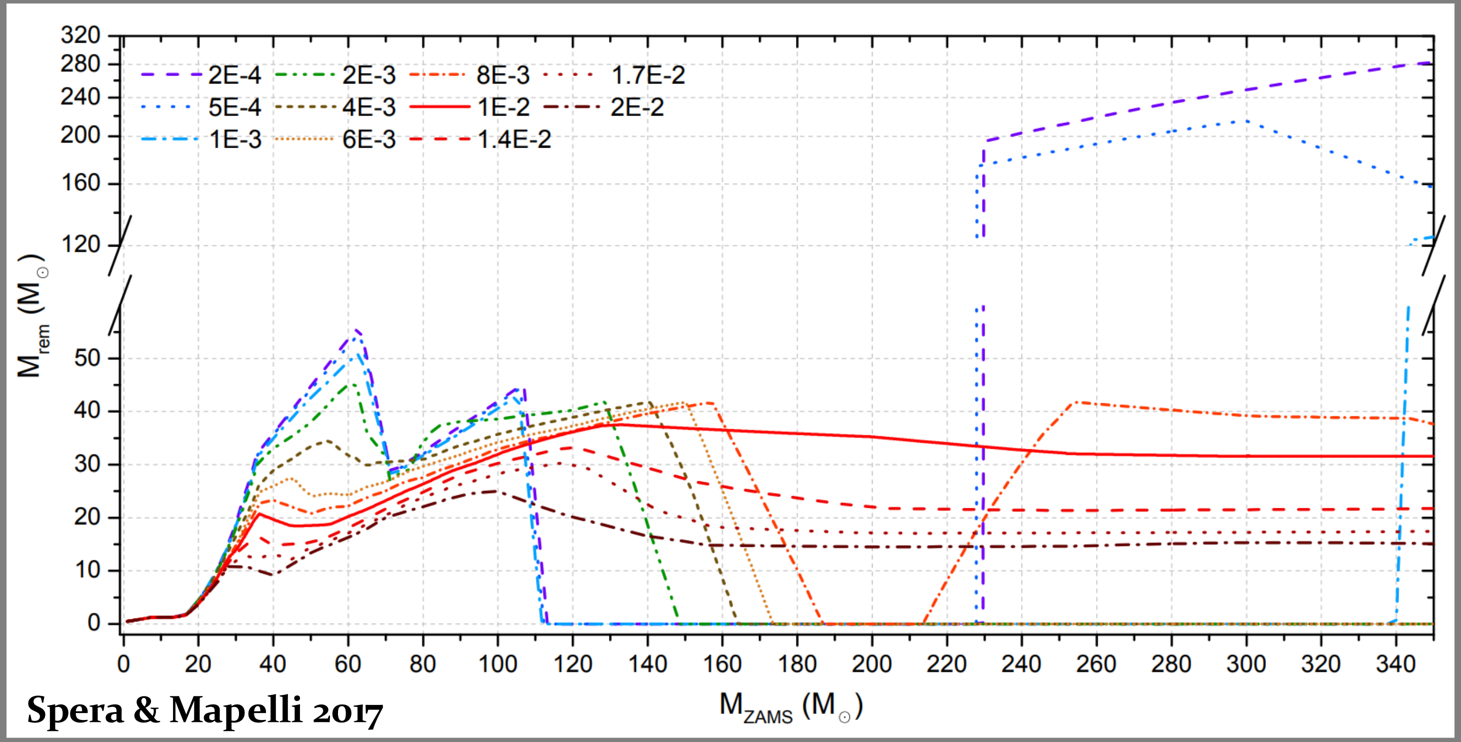

Spera & Mapelli 2017

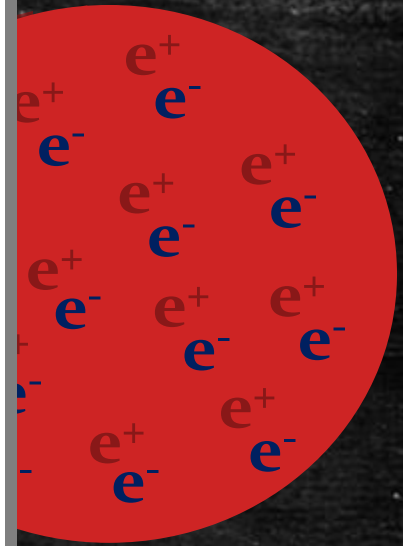

PPISN

PISN

DCBH

$100\ M_\odot$

$140\ M_\odot$

Heger & Woosley 2002
Heger et al. 2003

$260\ M_\odot$

$300\ M_\odot$

no PISN observations

only candidate identifications
(e.g. Super-Luminous Supernovae, SLSNe)

no PISN observations

only candidate identifications
(e.g. Super-Luminous Supernovae, SLSNe)

several hundreds CCSN observations

$$L_{PISN} \lesssim 10^2 \, L_{CCSN}$$

no PISN observations

only candidate identifications
(e.g. Super-Luminous Supernovae, SLSNe)

several hundreds CCSN observations

$L_{PISN} \lesssim 10^2 L_{CCSN}$

where are the PISNe?

no PISN observations

only candidate identifications
(e.g. Super-Luminous Supernovae, SLSNe)

several hundreds
CCSN observations

$$L_{PISN} \lesssim 10^2 \, L_{CCSN}$$

where are the PISNe?

intrinsically few

observational issues

no PISN observations

only candidate identifications
(e.g. Super-Luminous Supernovae, SLSNe)

several hundreds CCSN observations

$$L_{PISN} \lesssim 10^2 \, L_{CCSN}$$

where are the PISNe?

intrinsically few

observational issues

Aim

cosmic PISN rate density

$$\frac{dN_{PISN}}{dtdV}(z) = \int dZ \, \frac{dM_{SFR}}{dtdV\,dZ}(z, Z) \times \frac{dN_{PISN}}{dM_{SFR}}(Z)$$

Aim

cosmic PISN rate density

$$\frac{dN_{PISN}}{dtdV}(z) = \int dZ \frac{dM_{SFR}}{dtdV\,dZ}(z,Z) \times \frac{dN_{PISN}}{dM_{SFR}}(Z)$$

galaxy evolution model

stellar evolution simulations

explore dependence on

Methods

Galaxy semi-empirical model

Boco et al. 2021, Chruslinska et al. 2021, Popesso et al. 2022, Curti et al. 2020

Z-dependent Star Formation Rate Density

(SFRD)

$$\frac{dM_{SFR}(z, Z)}{dt\, dV\, dZ}$$

Boco et al. 2021, Chruslinska et al. 2021, Popesso et al. 2022, Curti et al. 2020

Galaxy semi-empirical model

Z-dependent Star Formation Rate Density

(SFRD)

$$\frac{dM_{SFR}(z, Z)}{dt\, dV\, dZ}$$

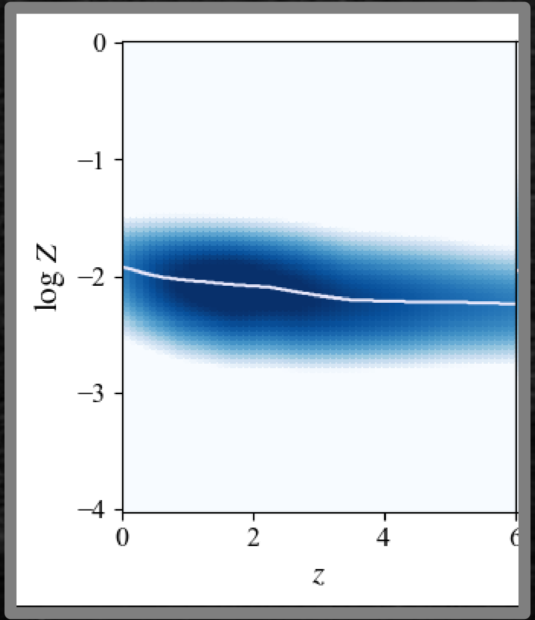

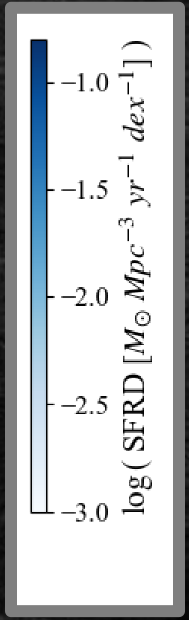

Boco et al. 2021, Chruslinska et al. 2021,
Popesso et al. 2022, Curti et al. 2020

Galaxy semi-empirical model

Z-dependent
Star Formation Rate Density
(SFRD)

$$\frac{dM_{SFR}(z,Z)}{dt\,dV\,dZ}$$

$$\sigma_Z = 0.15$$

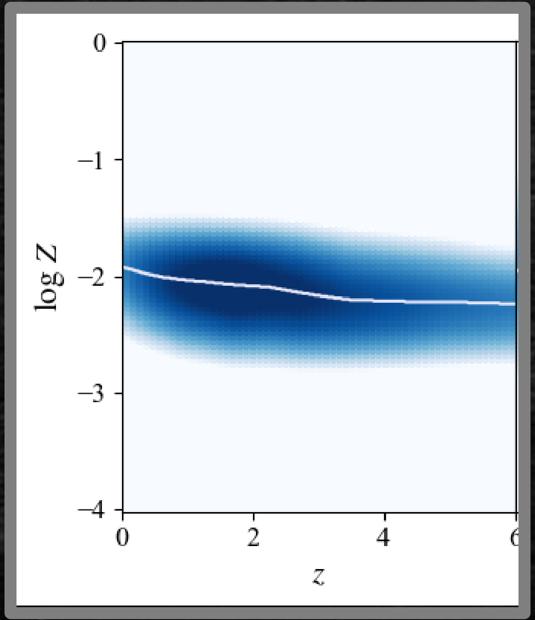

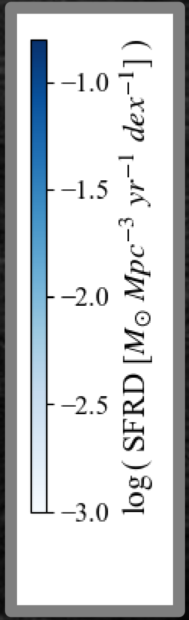

Boco et al. 2021, Chruslinska et al. 2021, Popesso et al. 2022, Curti et al. 2020

Galaxy semi-empirical model

Z-dependent
Star Formation Rate Density

(SFRD)

$$\frac{dM_{SFR}(z, Z)}{dt\, dV\, dZ}$$

$\sigma_Z = 0.15$ 0.35

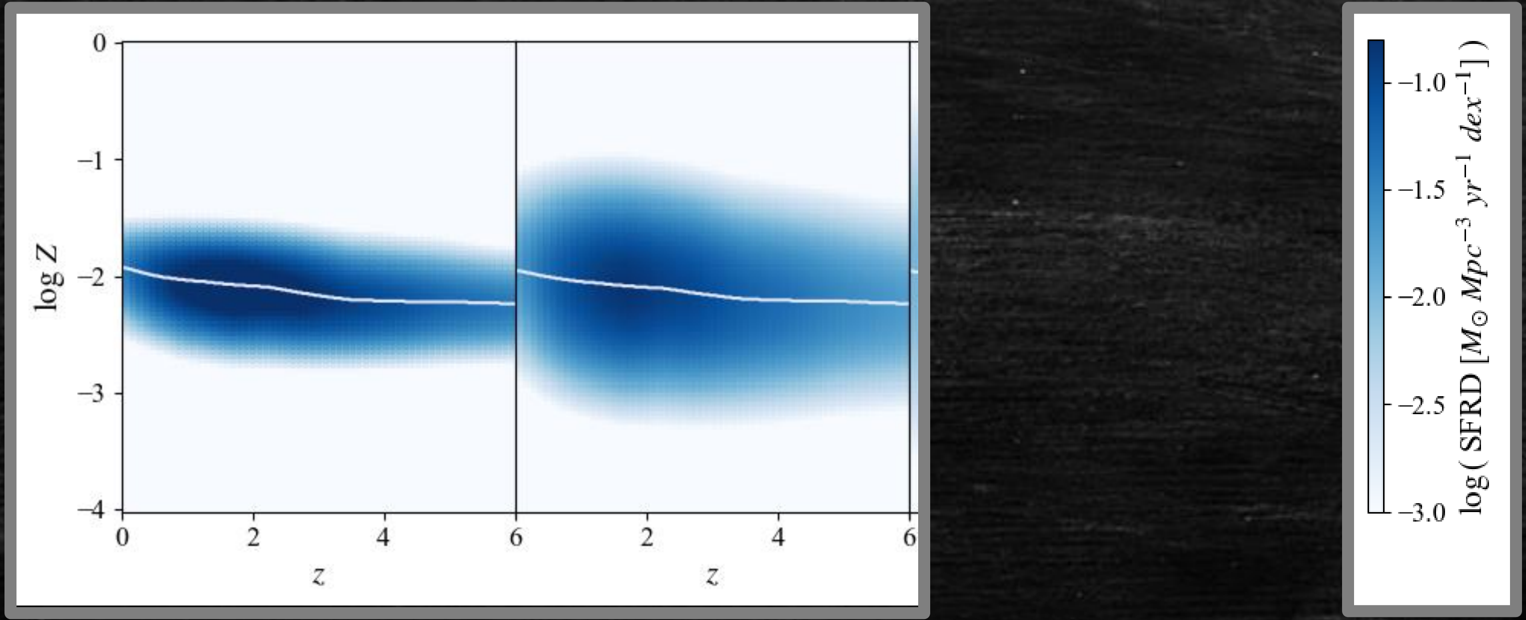

Boco et al. 2021, Chruslinska et al. 2021, Popesso et al. 2022, Curti et al. 2020

Galaxy semi-empirical model

Z-dependent Star Formation Rate Density (SFRD)

$$\frac{dM_{SFR}(z, Z)}{dt\, dV\, dZ}$$

$\sigma_Z = 0.15$ | 0.35 | 0.70

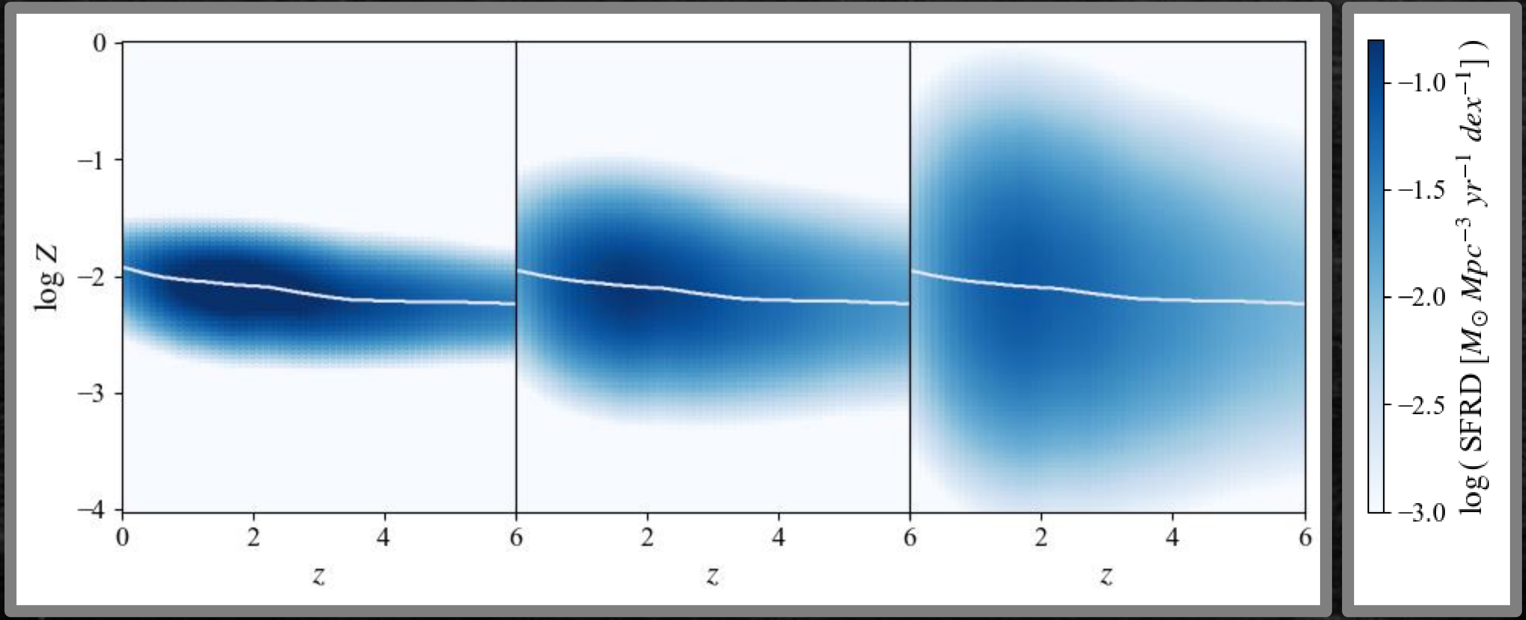

Boco et al. 2021, Chruslinska et al. 2021, Popesso et al. 2022, Curti et al. 2020

Galaxy semi-empirical model

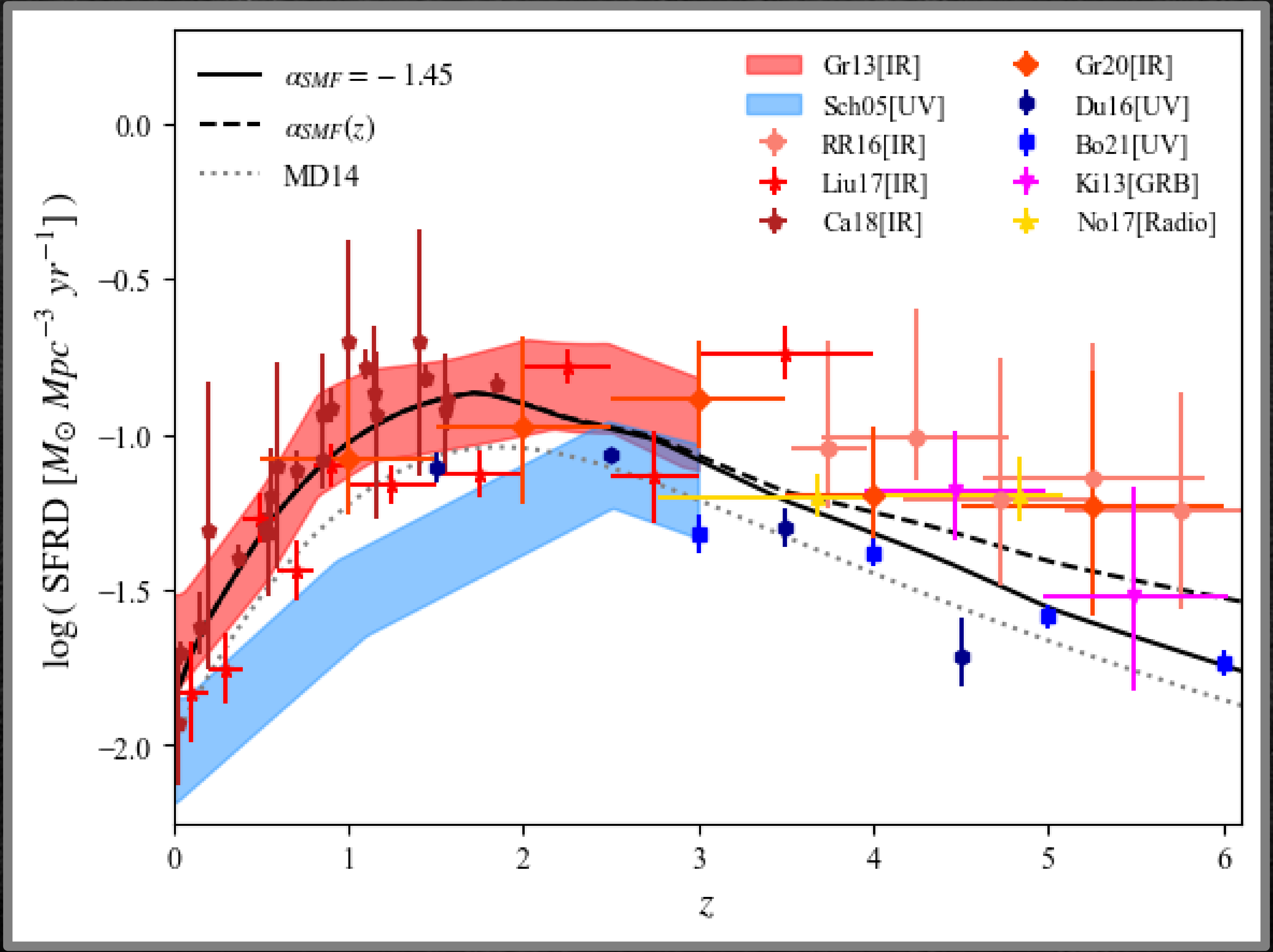

Stellar evolution model

$$\frac{dN_{PISN}}{dM_{SFR}}(Z) = \frac{\int_{M_{entry}(Z)}^{M_{exit}(Z)} \phi(M)\, dM}{\int_{0.1\,M_\odot}^{M_{up}} M\, \phi(M)\, dM}$$

Stellar evolution model

$$\frac{dN_{PISN}}{dM_{SFR}}(Z) = \frac{\int_{M_{entry}(Z)}^{M_{exit}(Z)} \phi(M)\, dM}{\int_{0.1\, M_\odot}^{M_{up}} M\, \phi(M)\, dM}$$

Kroupa IMF

$[0.1\, M_\odot\, ,\; M_{up}\,]$

$150\, M_\odot$

$300\, M_\odot$

Stellar evolution model

$$\frac{dN_{PISN}}{dM_{SFR}}(Z) = \frac{\int_{M_{entry}(Z)}^{M_{exit}(Z)} \phi(M)\, dM}{\int_{0.1\, M_\odot}^{M_{up}} M\, \phi(M)\, dM}$$

→ Kroupa IMF

$[0.1\, M_\odot\, ,\ M_{up}\,]$

$150\ M_\odot$

$300\ M_\odot$

$[45, 120]\ M_\odot$
$[55, 110]\ M_\odot$
$[60, 105]\ M_\odot$

M_{CO} → $M_{entry/exit}\,(Z)$

PARSEC — Bressan et al. 2012, Costa et al. 2019, 2021, Spera & Mapelli 2017, Iorio et al 2023

FRANEC — Chieffi & Limongi 2013, Limongi & Chieffi 2018

Stellar evolution model

single stars

$$\frac{dN_{PISN}}{dM_{SFR}}(Z) = \frac{\int_{M_{entry}(Z)}^{M_{exit}(Z)} \phi(M)\, dM}{\int_{0.1\,M_\odot}^{M_{up}} M\,\phi(M)\, dM}$$

Kroupa IMF

$[0.1\,M_\odot\,,\ M_{up}]$

$150\,M_\odot$

$300\,M_\odot$

$[45, 120]\,M_\odot$

$[55, 110]\,M_\odot$

$[60, 105]\,M_\odot$

M_{CO} → $M_{entry/exit}\,(Z)$

PARSEC

Bressan et al. 2012, Costa et al. 2019, 2021
Spera & Mapelli 2017, Iorio et al 2023

FRANEC

Chieffi & Limongi 2013, Limongi & Chieffi 2018

$$\frac{dN_{PISN}}{dM_{SFR}}(Z)$$

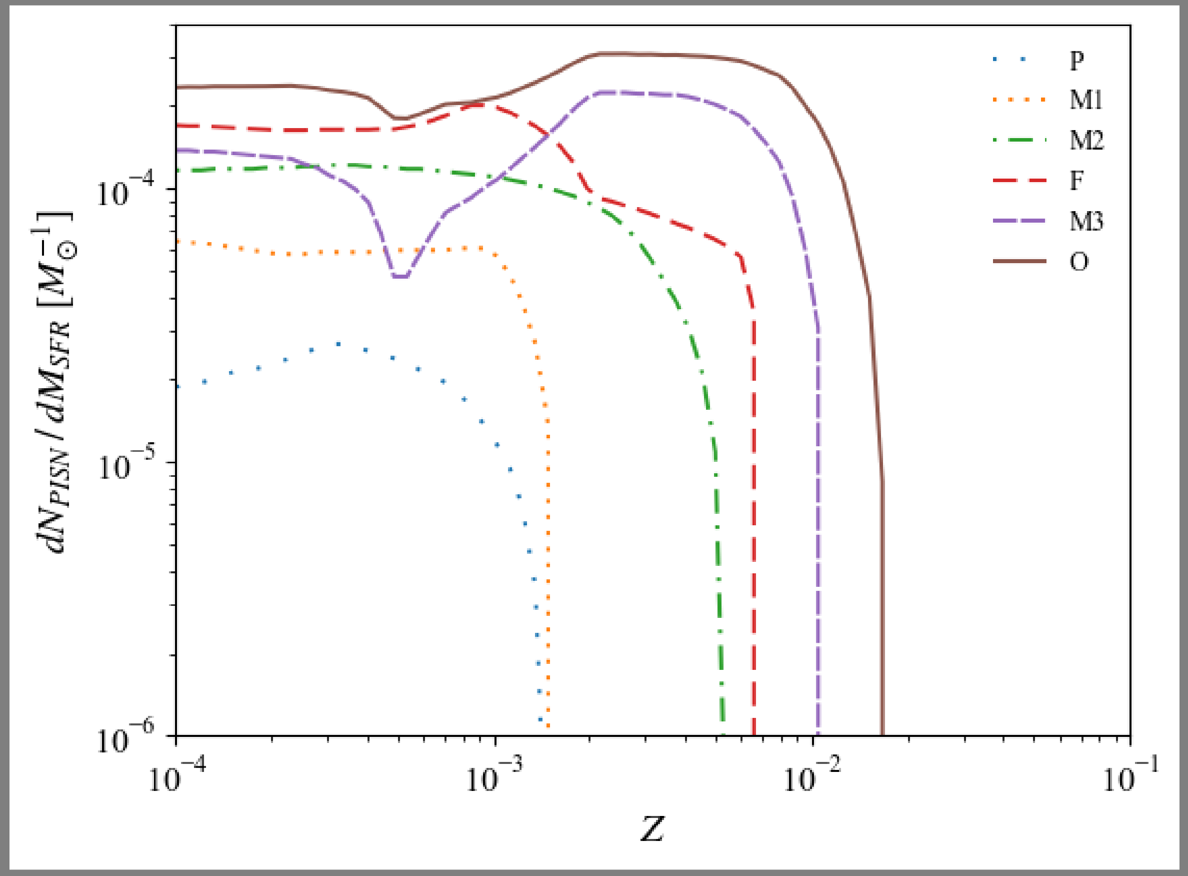

stellar variations

name	stellar code	$M_{CO}/M_\odot$	$M_{up}/M_\odot$	Z_{max}
P	FRANEC	60-105	150	1.5×10^{-3}
M1	PARSEC-I	55-110	150	1.5×10^{-3}
M2	FRANEC	45-120	150	5.5×10^{-3}
F	PARSEC-I	55-110	300	6.6×10^{-3}
M3	PARSEC-II	45-120	150	1.0×10^{-2}
O	PARSEC-II	45-120	300	1.7×10^{-2}

$$\frac{dN_{PISN}}{dM_{SFR}}(Z)$$

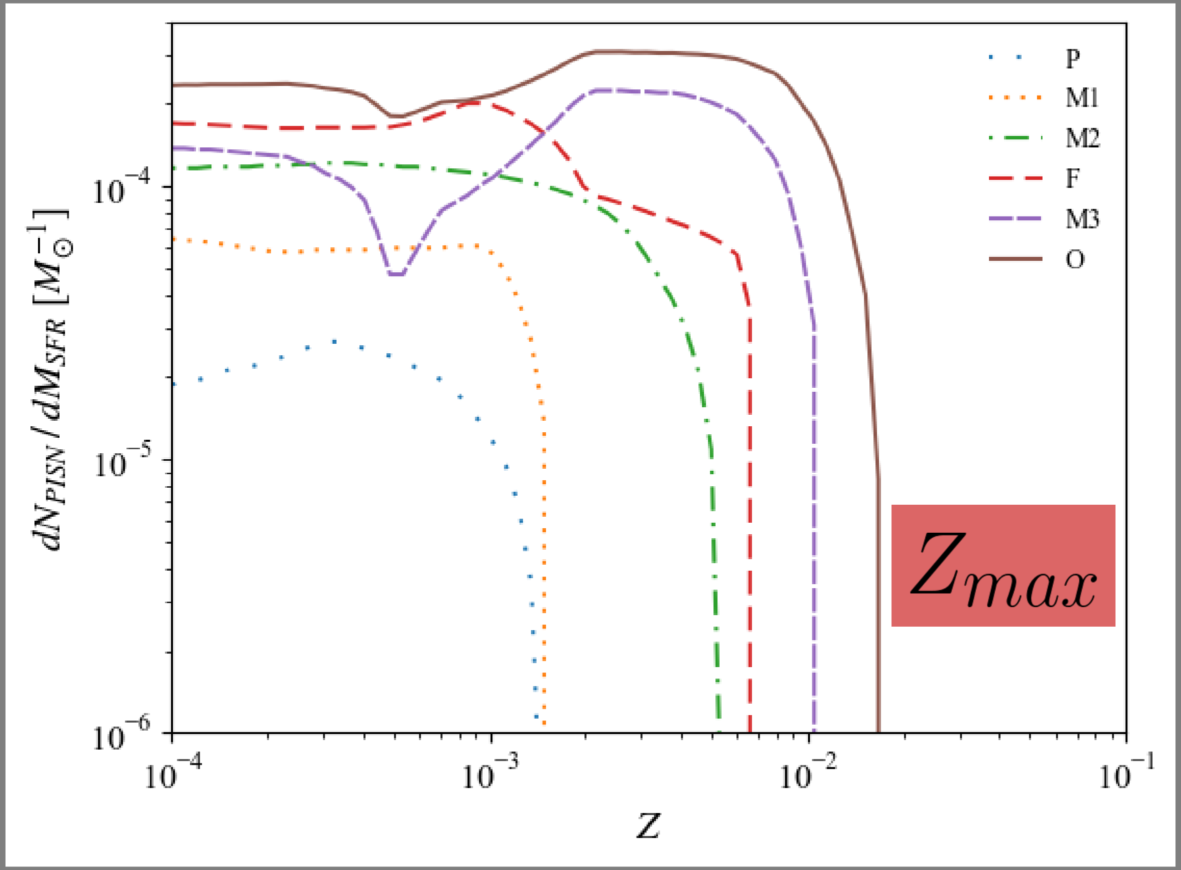

stellar variations

name	stellar code	$M_{CO}/M_\odot$	$M_{up}/M_\odot$	Z_{max}
P	FRANEC	60-105	150	1.5×10^{-3}
M1	PARSEC-I	55-110	150	1.5×10^{-3}
M2	FRANEC	45-120	150	5.5×10^{-3}
F	PARSEC-I	55-110	300	6.6×10^{-3}
M3	PARSEC-II	45-120	150	1.0×10^{-2}
O	PARSEC-II	45-120	300	1.7×10^{-2}

Results

stellar variations

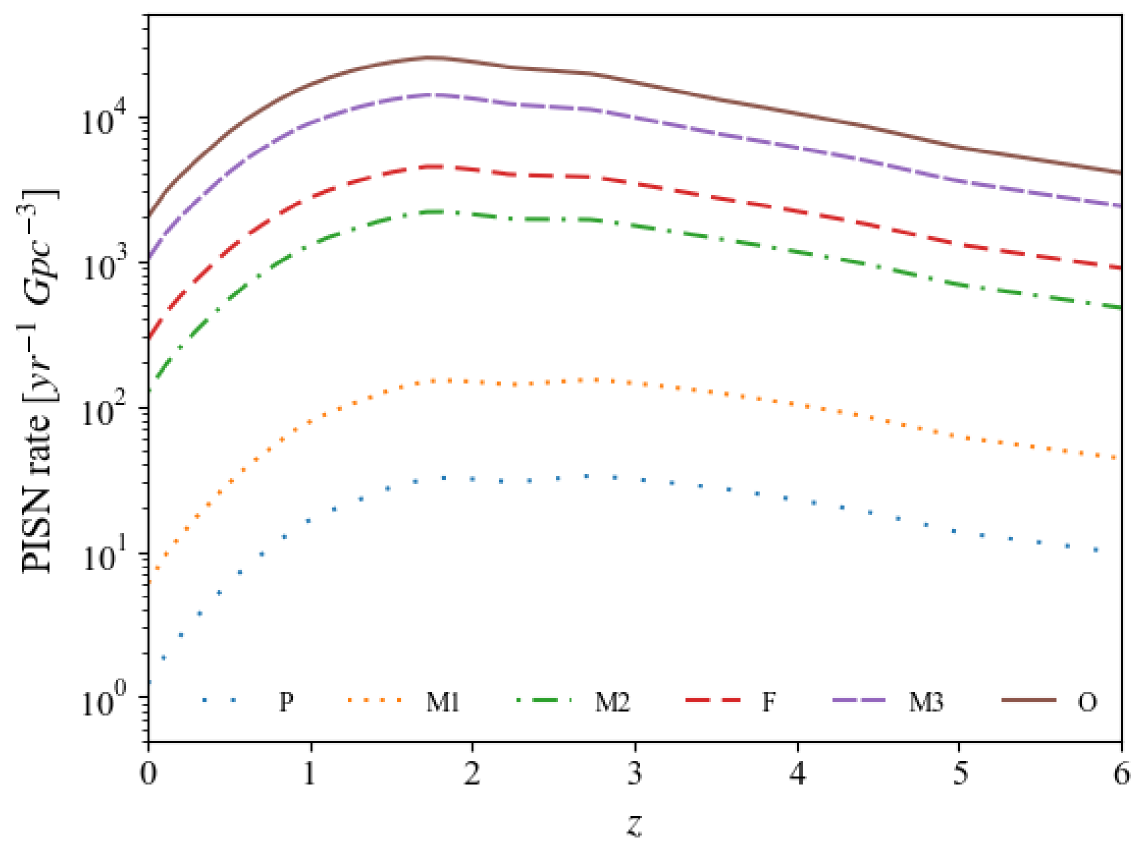

name	stellar code	$M_{CO}/M_\odot$	$M_{up}/M_\odot$	Z_{max}
P	FRANEC	60-105	150	1.5×10^{-3}
M1	PARSEC-I	55-110	150	1.5×10^{-3}
M2	FRANEC	45-120	150	5.5×10^{-3}
F	PARSEC-I	55-110	300	6.6×10^{-3}
M3	PARSEC-II	45-120	150	1.0×10^{-2}
O	PARSEC-II	45-120	300	1.7×10^{-2}

galactic variations

Z_{max} ⟷ σ_Z

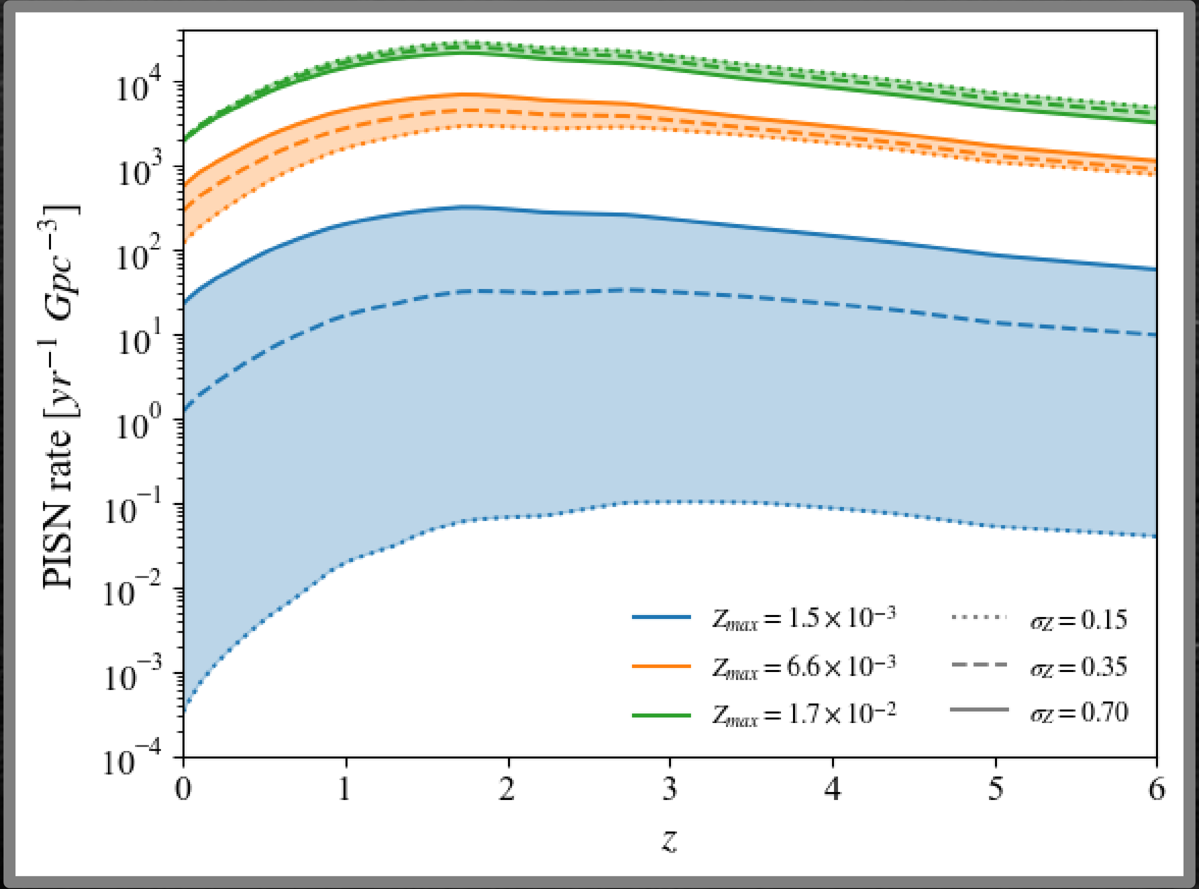

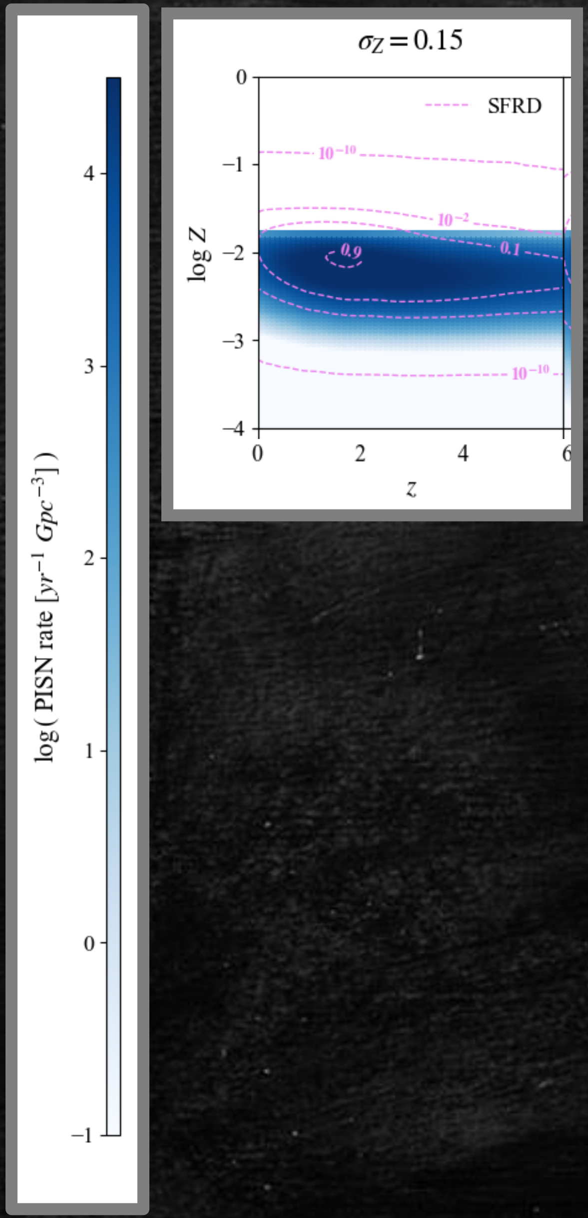
log(PISN rate [yr^-1 Gpc^-3])
4
3
2
1
0
−1
σZ = 0.15
SFRD
log Z
0
−1
−2
−3
−4
z
0
2
4
6
10^−10
10^−2
0.1
0.9
10^−10

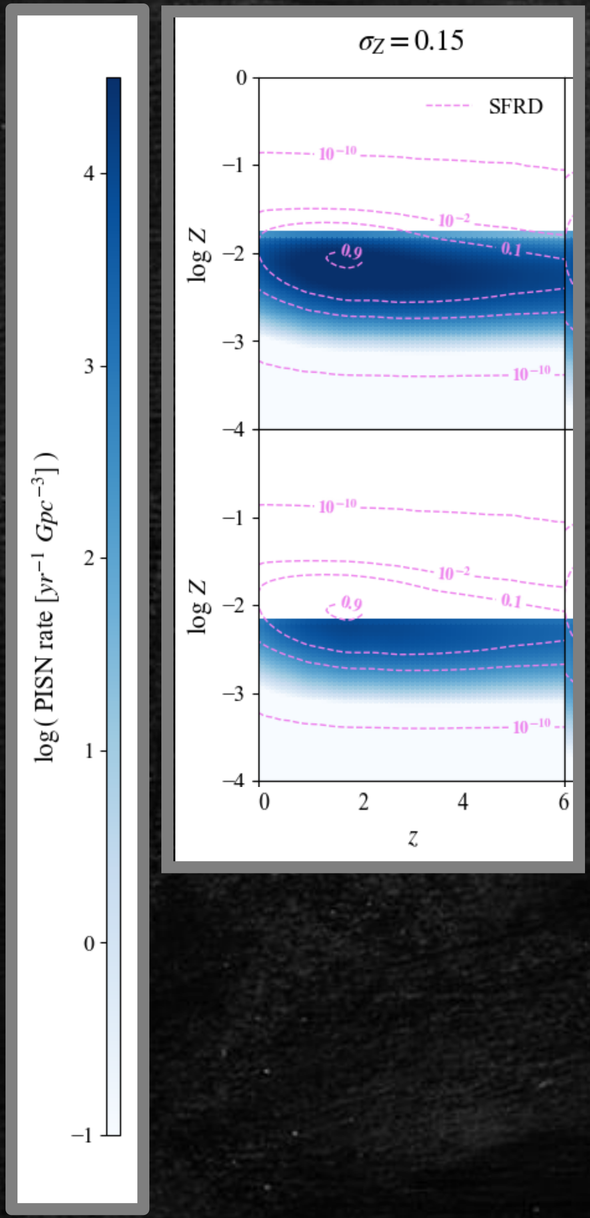

Z_{max}

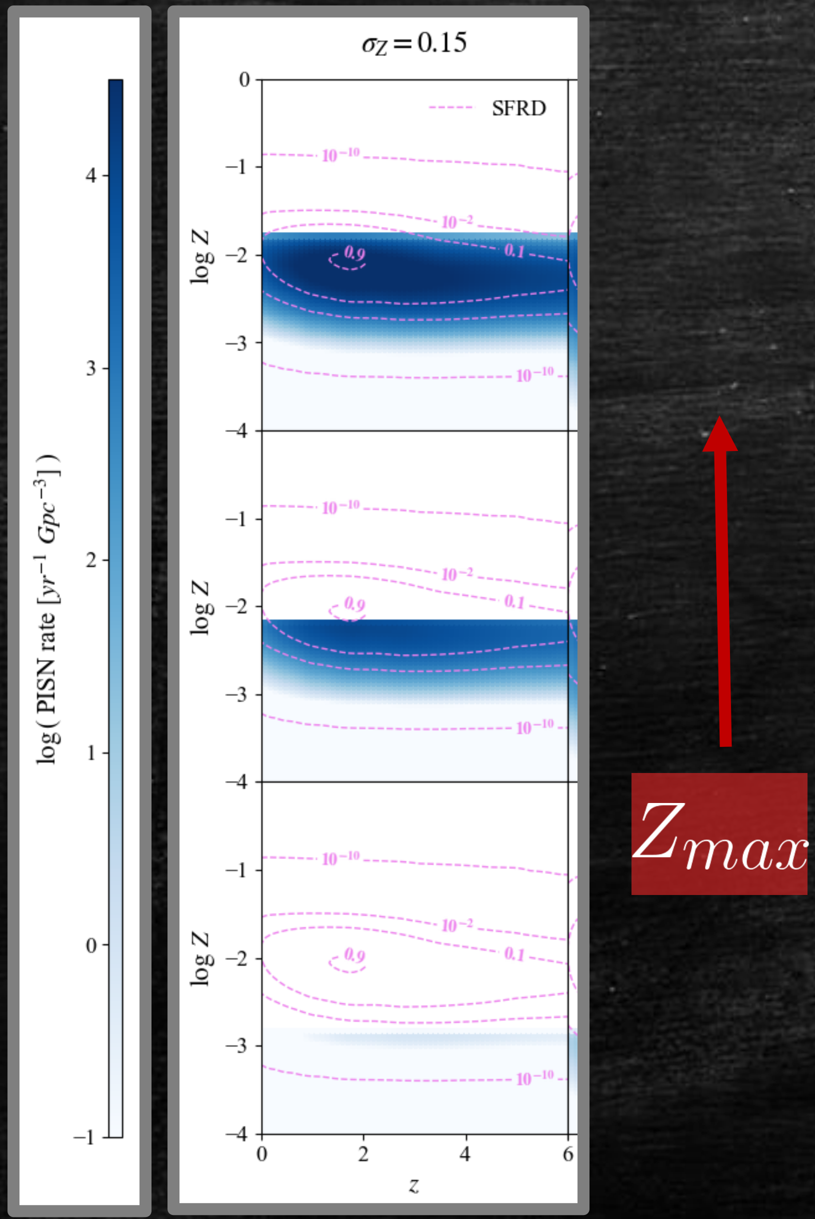

$\sigma_Z = 0.15$
SFRD
log Z
z
log(PISN rate [yr^{-1} Gpc^{-3}])
Z_{max}

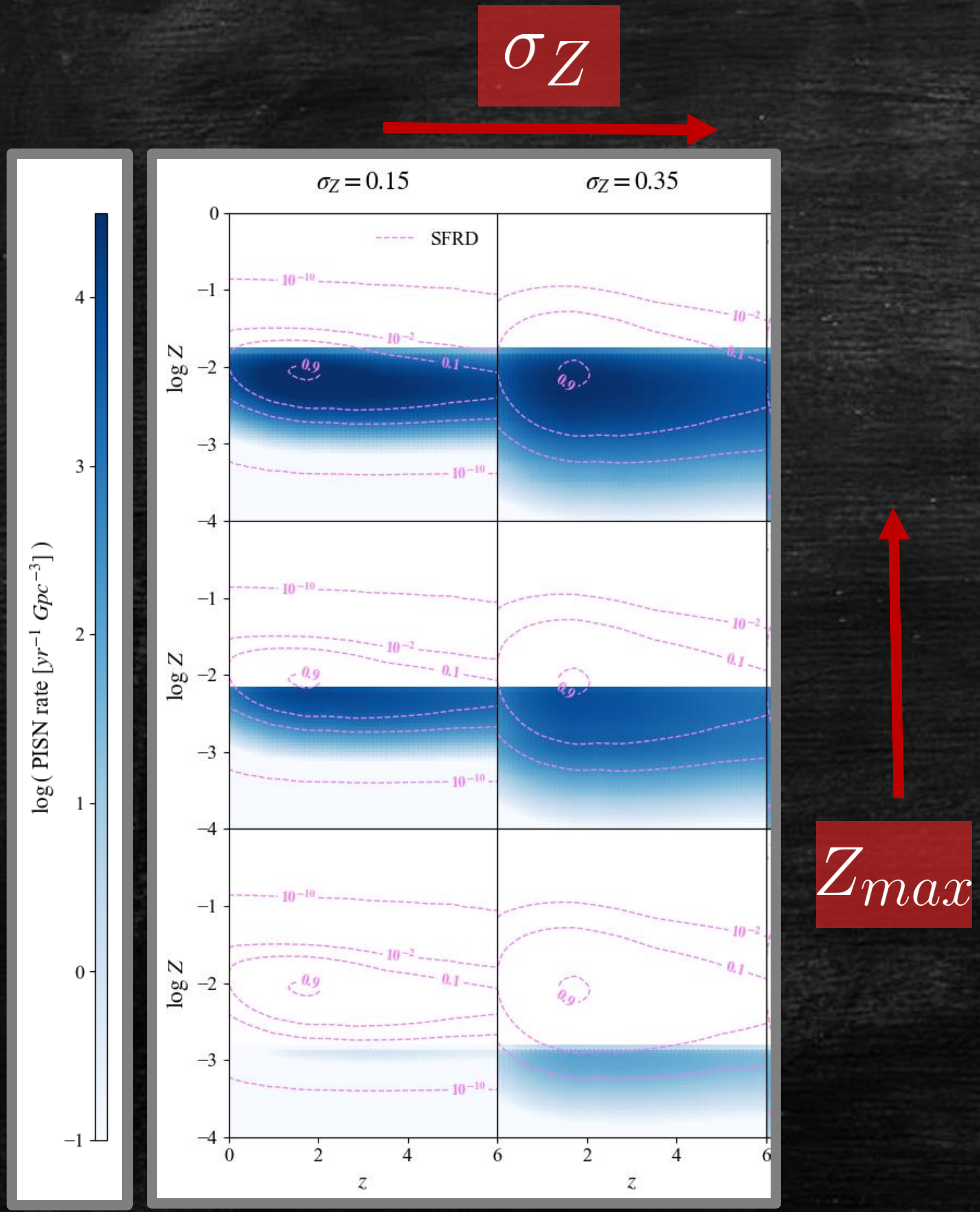
σ_Z
Z_{max}
$\sigma_Z = 0.15$
$\sigma_Z = 0.35$
SFRD
log(PISN rate $[yr^{-1}\ Gpc^{-3}]$)
log Z
z

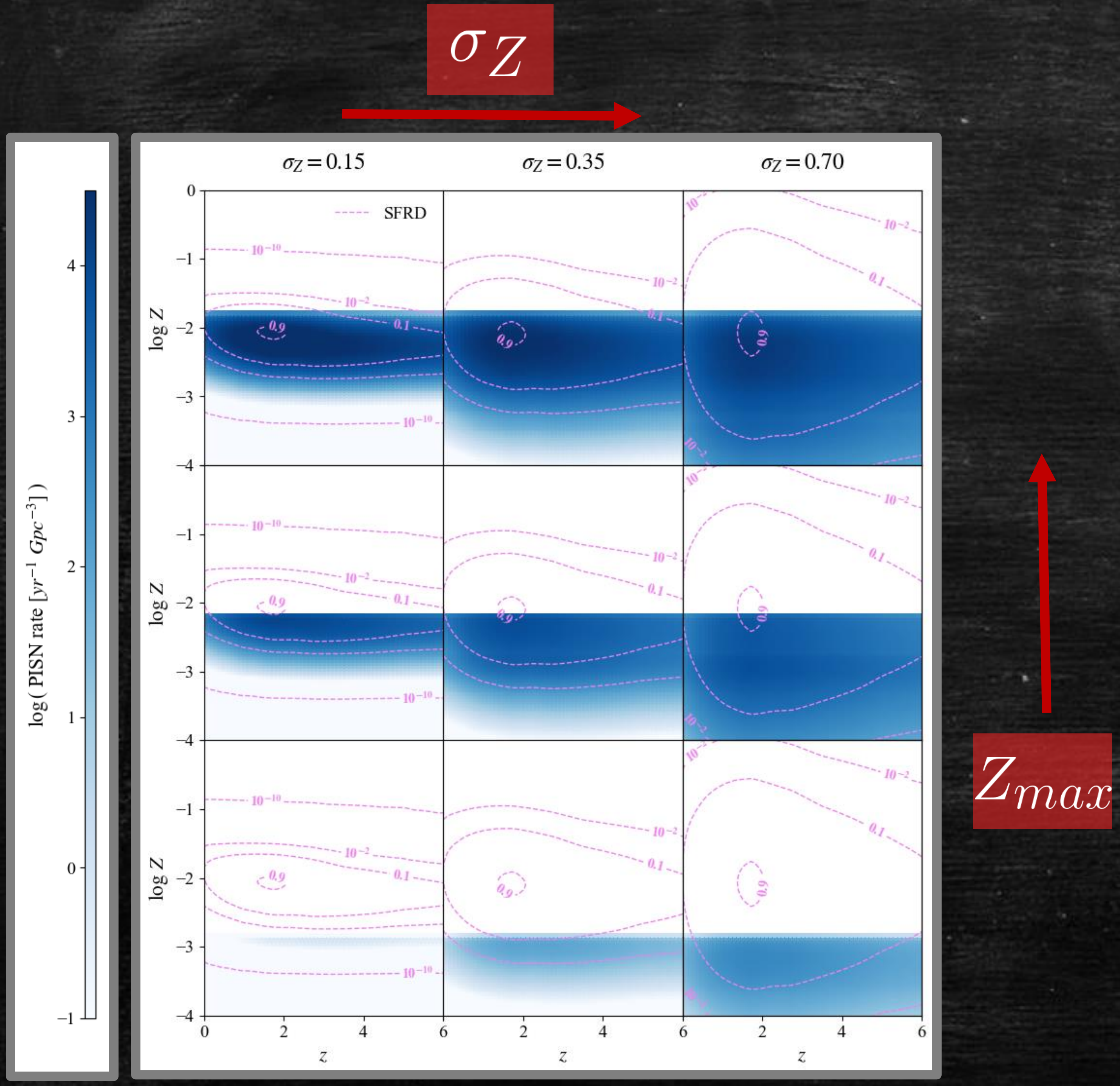

σ_Z
$\sigma_Z = 0.15$
$\sigma_Z = 0.35$
$\sigma_Z = 0.70$
SFRD
log Z
z
log(PISN rate $[yr^{-1}\ Gpc^{-3}]$)
Z_{max}

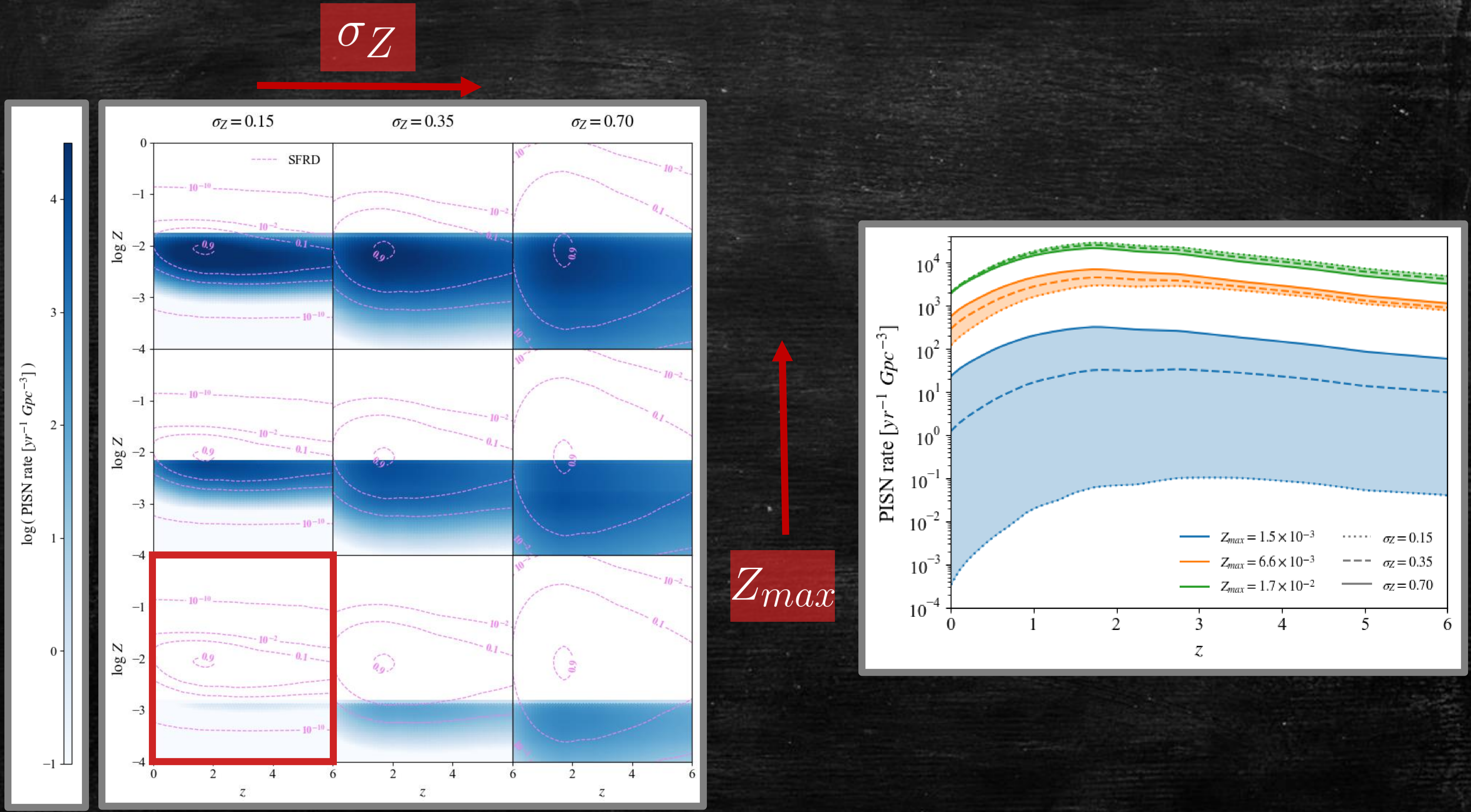

σ_Z
$\sigma_Z = 0.15$
$\sigma_Z = 0.35$
$\sigma_Z = 0.70$
SFRD
log Z
z
log(PISN rate [yr^{-1} Gpc^{-3}])
Z_{max}
PISN rate [yr^{-1} Gpc^{-3}]
$Z_{max} = 1.5 \times 10^{-3}$
$Z_{max} = 6.6 \times 10^{-3}$
$Z_{max} = 1.7 \times 10^{-2}$
$\sigma_Z = 0.15$
$\sigma_Z = 0.35$
$\sigma_Z = 0.70$

host galaxy properties

variation F

$\sigma_Z = 0.15$

$M_\star \sim 10^9 - 10^{10}\, M_\odot$

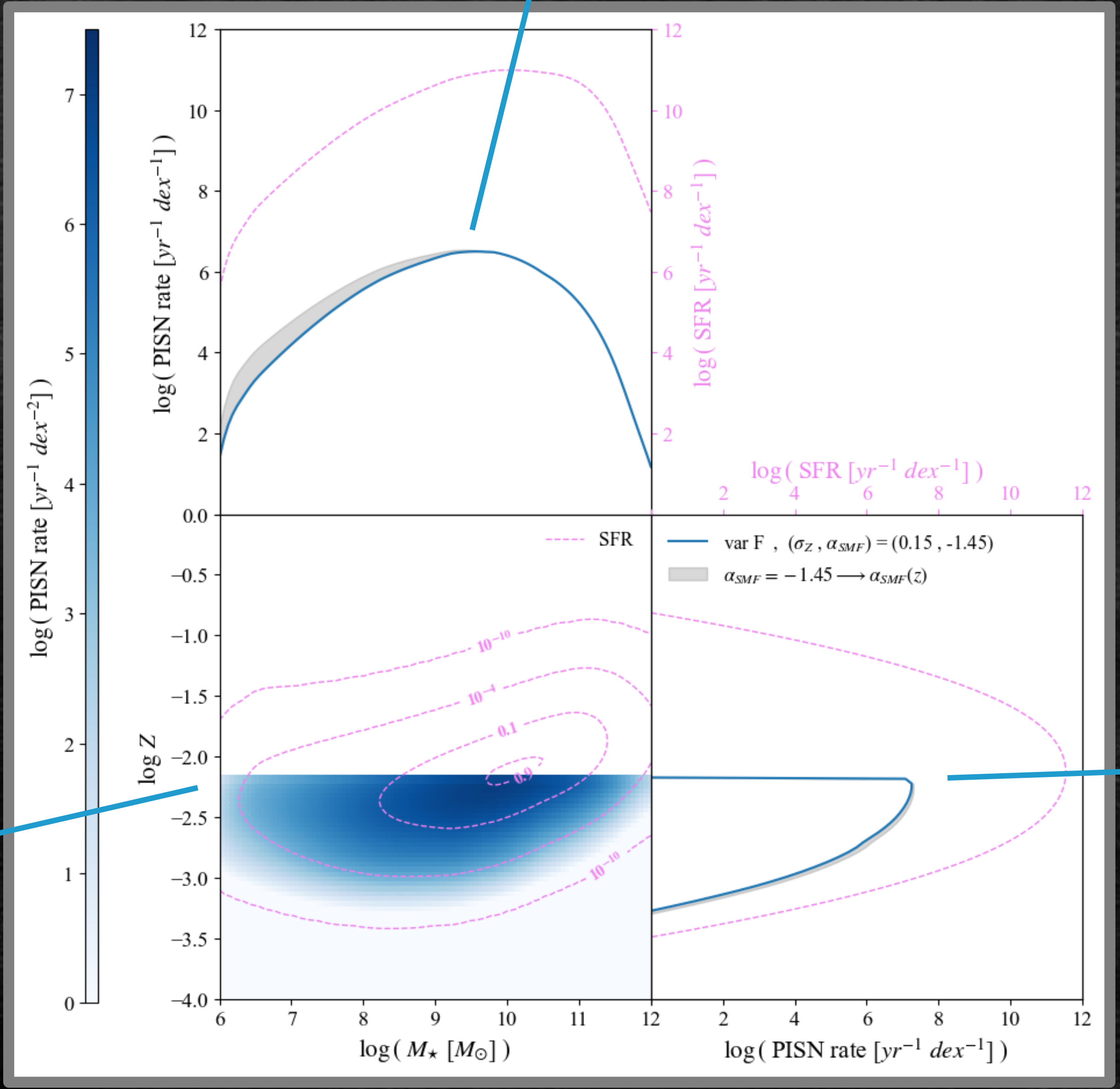

$Z \lesssim Z_{max}$

$Z_{max} = 8 \times 10^{-3}$

variation P
$\sigma_Z = 0.15$

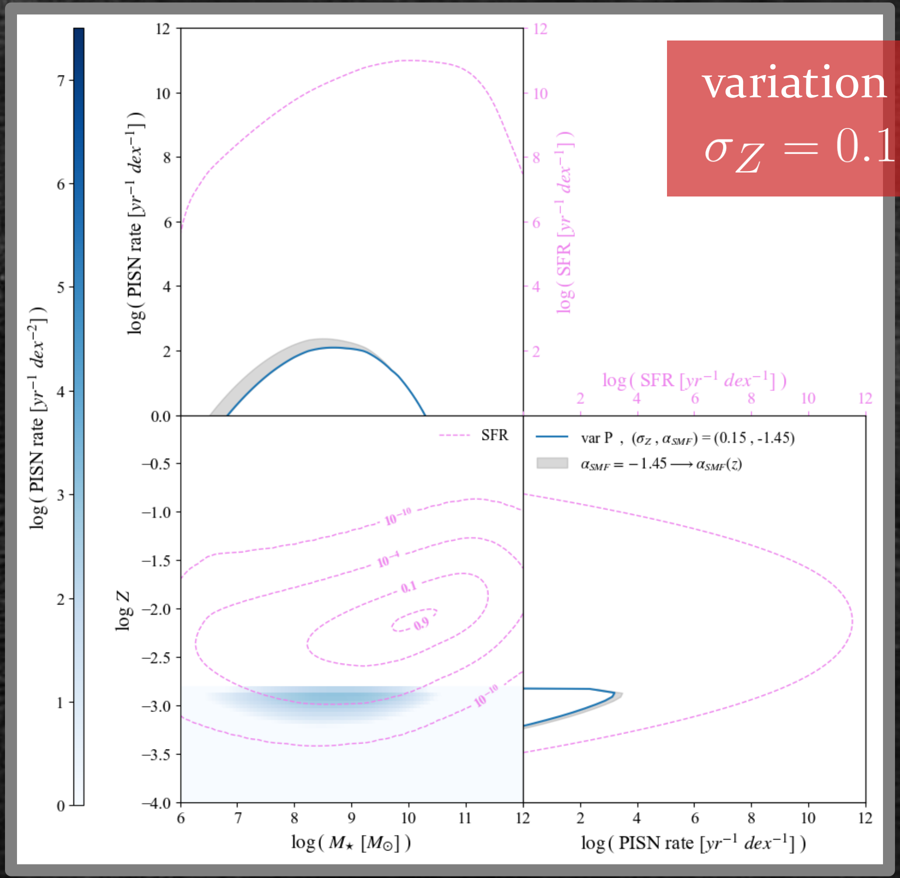

variation O
$\sigma_Z = 0.35$

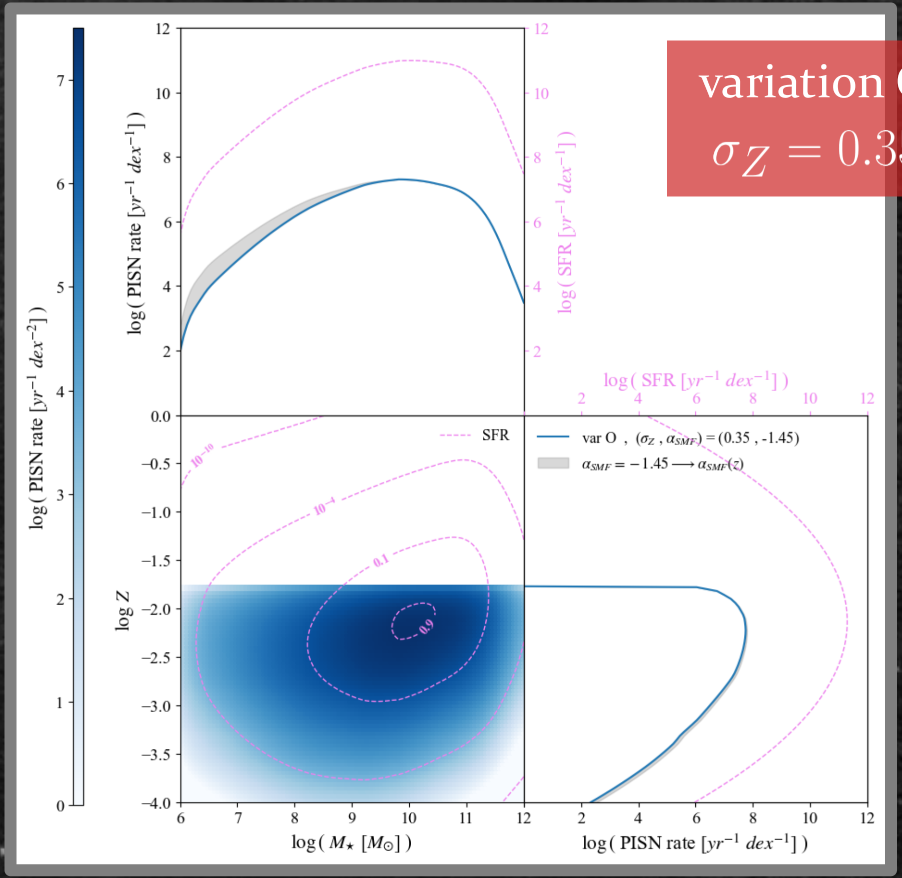

peak of PISN rate at
$Z \sim 10^{-3} - 10^{-2}$

→ Pop II stars main PISN progenitors, not Pop III

CAVEAT: SFRD and IMF at high z highly uncertain

PISNe in binaries

PARSEC
(Bressan et al. 2012, Costa et al. 2019, 2021)

SEVN
(Spera & Mapelli 2017, Iorio et al. 2023)

population of single stars

population of binaries

$$f_{bin} = 0.50$$

PISNe in binaries

PARSEC
(Bressan et al. 2012, Costa et al. 2019, 2021)

SEVN
(Spera & Mapelli 2017, Iorio et al. 2023)

population of single stars

population of binaries

$$f_{bin} = 0.50$$

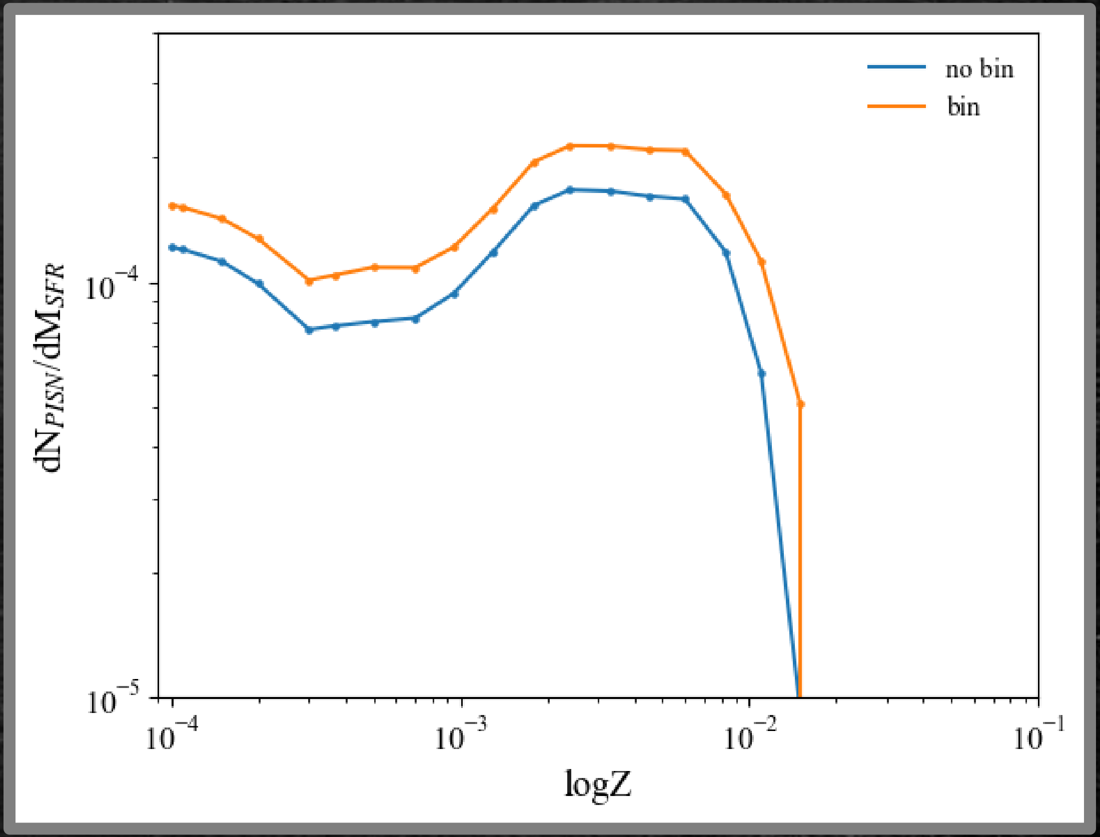

$$f_{bin}^{PISN} = 0.56$$

Conclusions

strong dependence on
stellar and galactic variations

→ PISN rate down to $\sim 10^{-4}/\mathrm{yr\ Gpc}^3 \quad (z=0)$

↓

intrinsically few

Conclusions

strong dependence on stellar and galactic variations → PISN rate down to $\sim 10^{-4}/\text{yr Gpc}^3 \quad (z=0)$

↓

intrinsically few

possible (or lack of) future PISN observations could pose constraints on

→

- maximum stellar Z to have PISN
- upper limit of stellar IMF
- dispersion of galaxy Z distribution in z

main contribution to PISN rate from $Z \sim 10^{-3} - 10^{-2}$

→ Pop II stars main PISN progenitors, not Pop III

main contribution to PISN rate from $Z \sim 10^{-3} - 10^{-2}$

→ Pop II stars main PISN progenitors, not Pop III

PISN contribution from binaries similar to single stars

main contribution to PISN rate from $Z \sim 10^{-3} - 10^{-2}$

→ Pop II stars main PISN progenitors, not Pop III

PISN contribution from binaries similar to single stars

single galaxy ($M_\star$, Z , ψ , z) contribution to PISN rate

↓

possible indications to future observational campaigns from host galaxy properties

where are the PISNe?

intrinsically few

observational issues

PISN detection rate

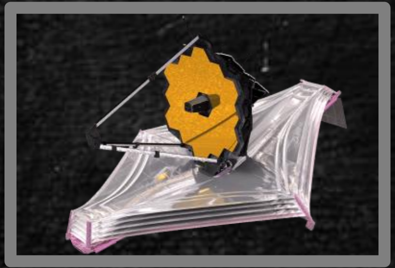

James Webb Space Telescope

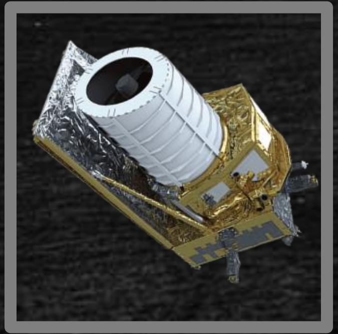

Euclid

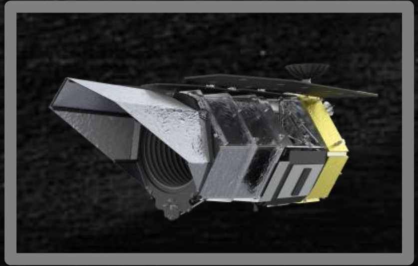

Nancy Grace Roman Space Telescope

Vera Rubin Observatory

ULTIMATE-Subaru

Zwicky Transient Facility

Back-up slides

Possible reasons for missed observation

assuming theory of stellar evolution is correct

PISNe only at high z (low Z environments) → too dim to be observed

stellar Initial Mass Function (IMF) does not extend up to PISN range

stars with mass > 300 $M_\odot$ observed (stellar mergers?)

PISNe preferentially in dusty environments → emission blocked by dust

PISNe more rare than CCSNe

PISN emission

early times

conversion of kinetic and radiation energy into thermal energy

later times

large amounts of radioactive ^{56}Ni up to $\sim 60\, M_\odot$

near-infrared band

expected PISN luminosity

$$L_{PISN} \lesssim 10^{44}\, erg/s$$

typical luminosity of Core-Collapse Supernovae (CCSNe) routinely observed in Local Universe

$$L_{CCSN} \sim 10^{42}\, erg/s$$

Galaxy semi-empirical model

Boco et al. 2021, Chruslinska et al. 2021, Popesso et al. 2022, Curti et al. 2020

Galaxy Stellar Mass Functions (GSMF)

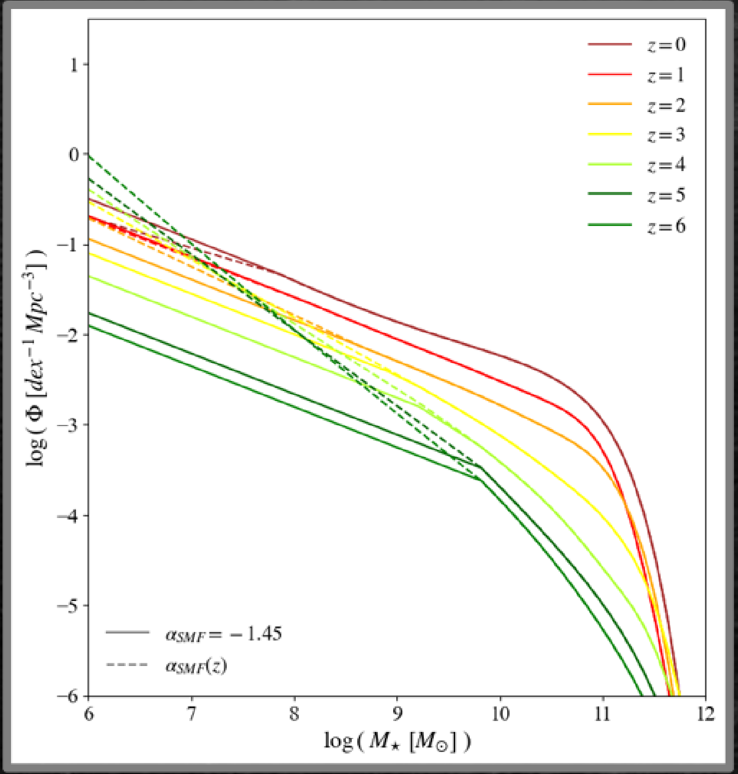

Davidson et al. 2017, Weaver et al. 2023

Galaxy Main Sequence (MS)

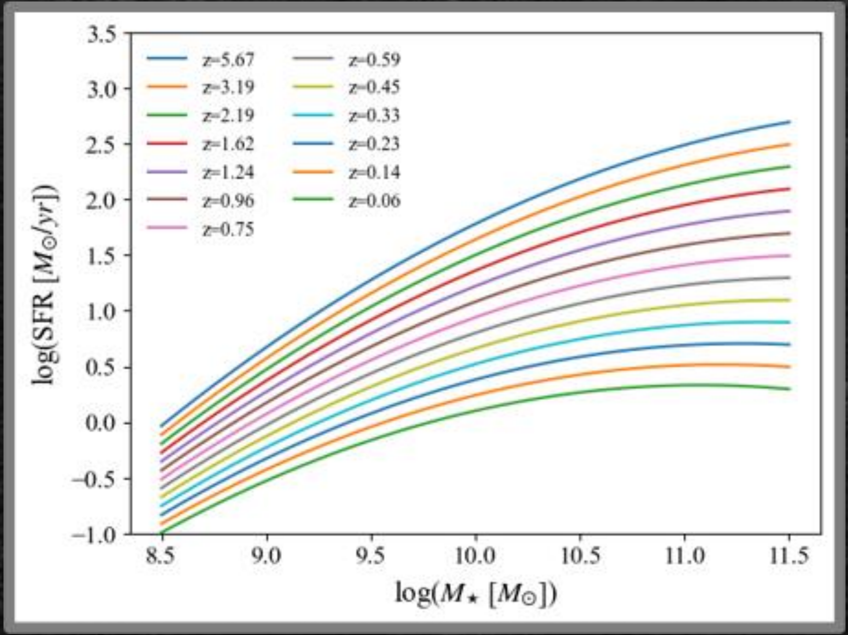

Speagle et al. 2014, Popesso et al. 2023

Fundamental Metallicity Relation (FMR)

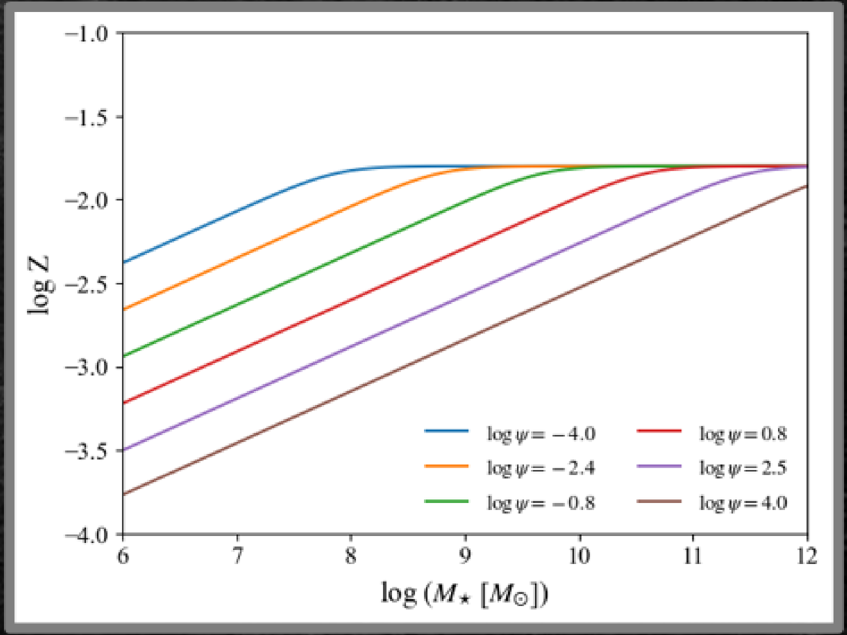

Mannucci et al. 2010, Curti et al. 2020, 2023

Galaxy Stellar Mass Functions

Chruslinska and Nelemans 2019

↓

analytical fits to observations

$$\Phi(M_\star) \propto e^{-M_\star/M_c} \left(\frac{M_\star}{M_c}\right)^{\alpha_{GSMF}}$$

combine several determinations

low-mass end slope

$$\alpha_{GSMF} = -1.45$$
$$= -0.1z - 1.34$$

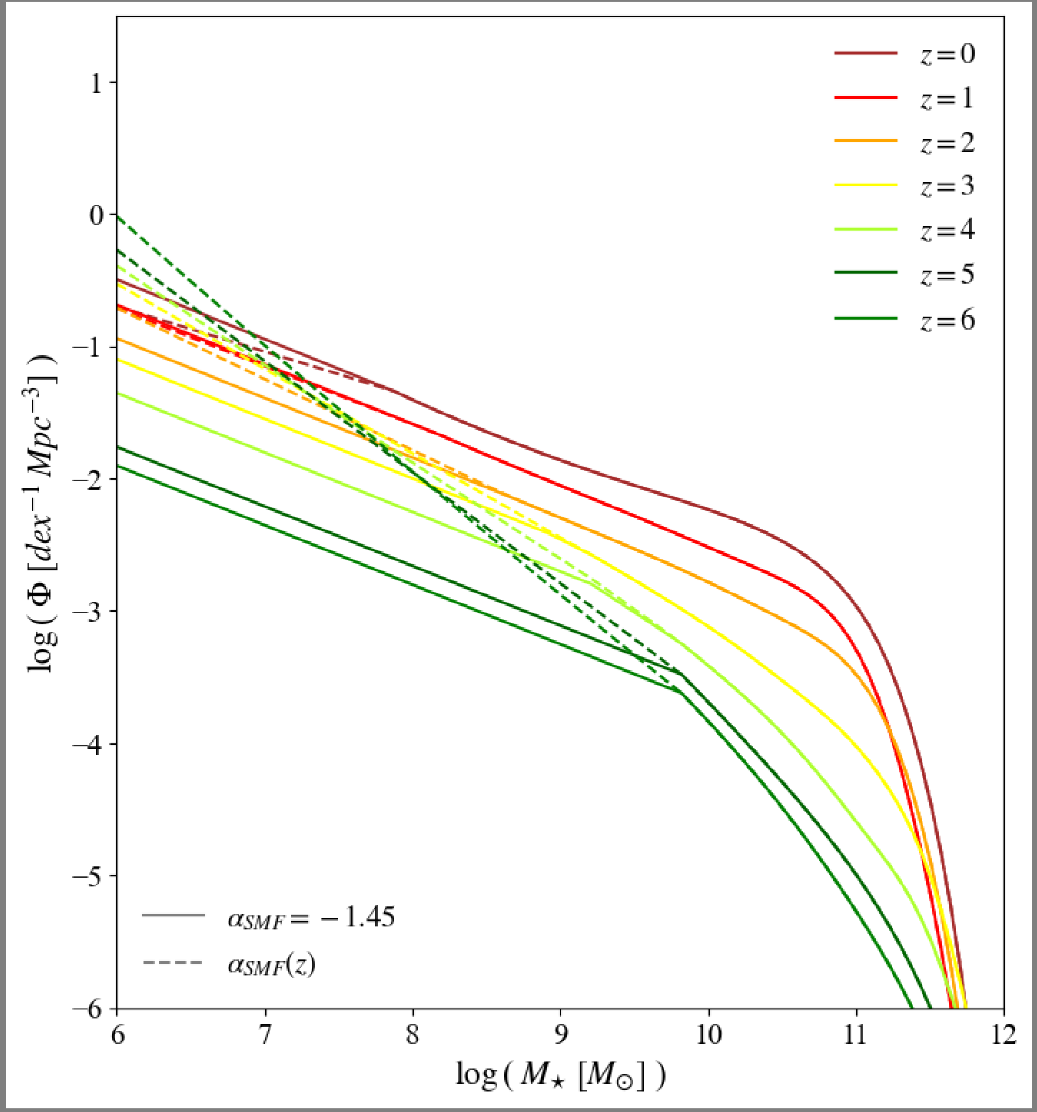

Galaxy Main Sequence

$$\frac{dp}{d\log\psi}(\psi, M_\star, z) = \frac{f_{MS}}{\sigma_{MS}\sqrt{2\pi}}\exp\left[-\frac{(\log\psi - \langle\log\psi\rangle_{MS})^2}{2\sigma_{MS}^2}\right] + \frac{f_{SB}}{\sigma_{SB}\sqrt{2\pi}}\exp\left[-\frac{(\log\psi - \langle\log\psi\rangle_{SB})^2}{2\sigma_{SB}^2}\right]$$

Popesso et al. 2022

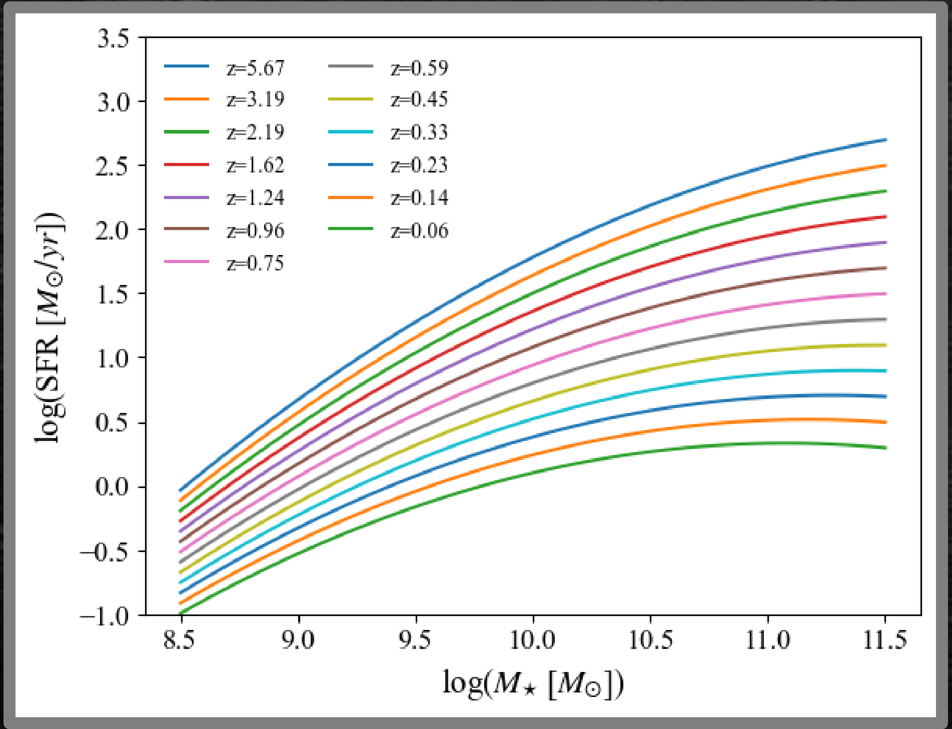

$$\log\psi = (-27.58 + 0.26t) + (4.95 - 0.04t)\log M_\star - 0.2(\log M_\star)^2$$

Chruslinska et al. 2021

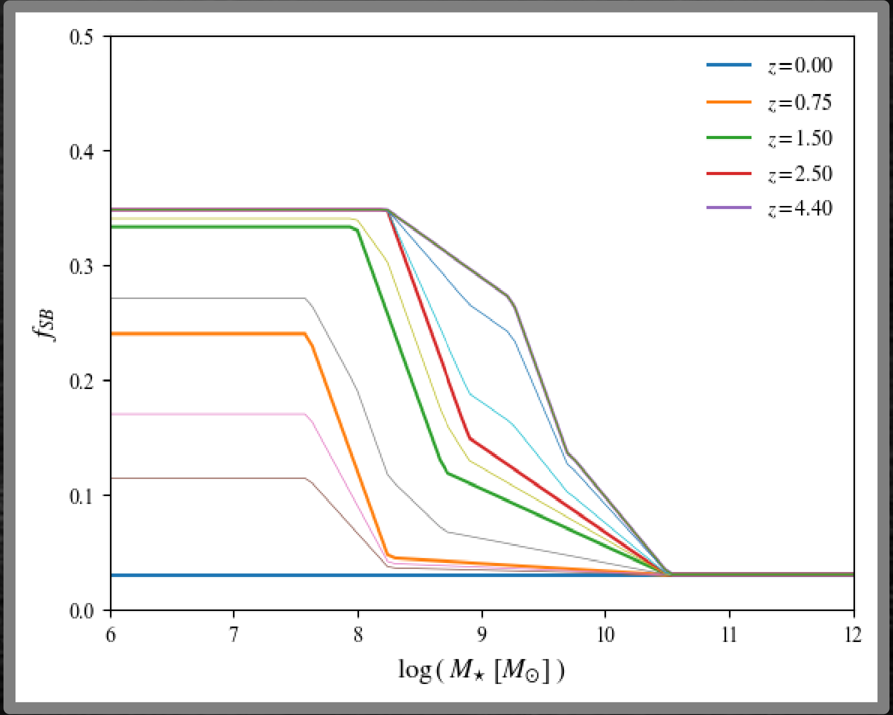

$$f_{MS} + f_{SB} = 1$$

$$\langle\log\psi\rangle_{SB} = \langle\log\psi\rangle_{MS} + 0.59$$

$$\sigma_{MS} = 0.188 \quad \sigma_{SB} = 0.243$$

Z evolution

$$Z_{FMR}(M_\star, \psi)$$

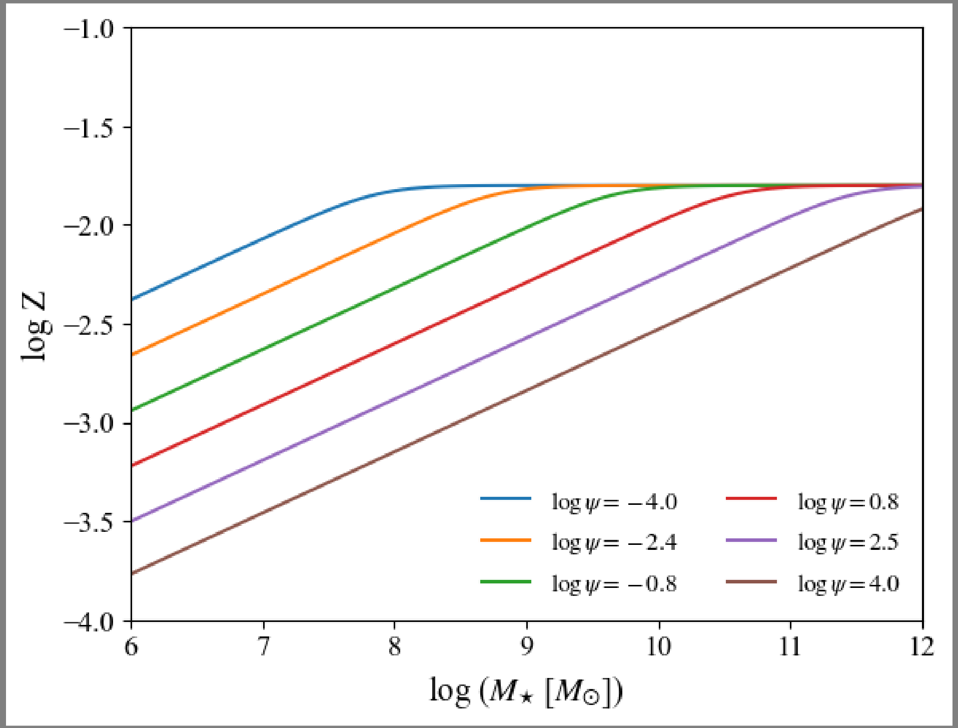

Curti et al. 2020

$$Z(\mathrm{M,SFR}) = Z_0 - \gamma/\beta \log(1 + (\mathrm{M/M_0(SFR)})^{-\beta})$$

$$\log(\mathrm{M_0(SFR)}) = m_0 + m_1 \log(\mathrm{SFR})$$

Z_0	m_0	m_1	γ	β
8.779 ± 0.005	10.11 ± 0.03	0.56 ± 0.01	0.31 ± 0.01	2.1 ± 0.4

$$\log Z = 12 + \log(\mathrm{O/H}) - 10.58$$

$$\frac{dp}{d\log Z}(Z, Z_{FMR}) \propto \exp\left[-\frac{(\log Z - \log Z_{FMR})^2}{2\sigma_Z^2}\right]$$

$$\sigma_Z = [0.15, 0.35, 0.70]$$

$M_{entry/exit}$ ranges

M_{CO} \ Z	1×10^{-4}	1×10^{-3}	4×10^{-3}	8×10^{-3}	1×10^{-2}	2×10^{-2}
			PARSEC-I			
45-120	108-257	109-435	158-458	178-222	-	-
55-110	126-237	128-382	195-415	-	-	-
60-105	138-228	139-355	213-394	-	-	-
			PARSEC-II			
45-120	107-229	112-239	92-221	111-294	133-366	-
55-110	117-150 153-211	130-227	109-202	138-270	166-335	-
60-105	125-145 158-203	140-221	118-193	151-258	182-320	-
			FRANEC			
45-120	111-262	113-272	136-415	183-565	220-600	-
55-110	131-242	134-251	173-378	233-514	282-600	-
60-105	141-232	145-240	192-360	259-488	313-592	-

$$\alpha_{GSMF} = -1.45 \longrightarrow \alpha_{GSMF}(z)$$

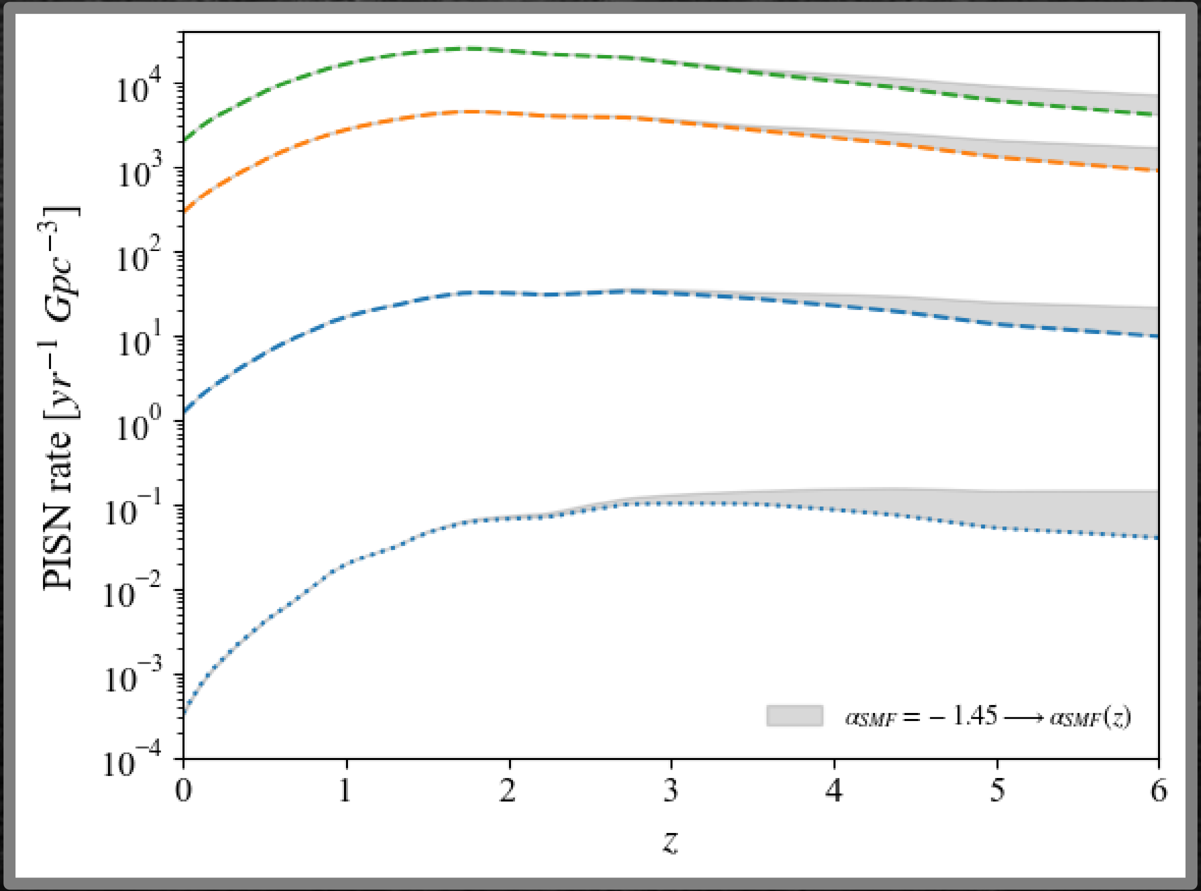

PISN / CCSN ratio

$$\frac{dN_{CCSN}}{dM_{SFR}} = \frac{\int_{8\,M_\odot}^{50\,M_\odot} \phi(M)\, dM}{\int_{0.1\,M_\odot}^{M_{up}} M\, \phi(M)\, dM}$$

σ_Z	PI/CC ($z = 0$)	PI/CC ($z = z^{\rm PI}_{\rm peak}$)	PI/CC ($z = 6$)
variation *P* ($Z_{\rm max} = 1.5 \times 10^{-3}$)			
0.15	2.5×10^{-9}	1.4×10^{-7}	2.3×10^{-7}
0.35	9.2×10^{-6}	3.5×10^{-5}	5.5×10^{-5}
0.70	1.7×10^{-4}	2.4×10^{-4}	3.3×10^{-4}
variation *F* ($Z_{\rm max} = 6.6 \times 10^{-3}$)			
0.15	9.2×10^{-4}	2.3×10^{-3}	4.5×10^{-3}
0.35	2.2×10^{-3}	3.5×10^{-3}	5.2×10^{-3}
0.70	4.3×10^{-3}	5.4×10^{-3}	6.6×10^{-3}
variation O ($Z_{\rm max} = 1.7 \times 10^{-2}$)			
0.15	1.5×10^{-2}	2.2×10^{-2}	2.8×10^{-2}
0.35	1.5×10^{-2}	2.0×10^{-2}	2.4×10^{-2}
0.70	1.5×10^{-2}	1.7×10^{-2}	1.9×10^{-2}

Host galaxy properties

$M_\star \sim 10^8 - 10^9 \, M_\odot$

variation P

$\sigma_Z = 0.15$

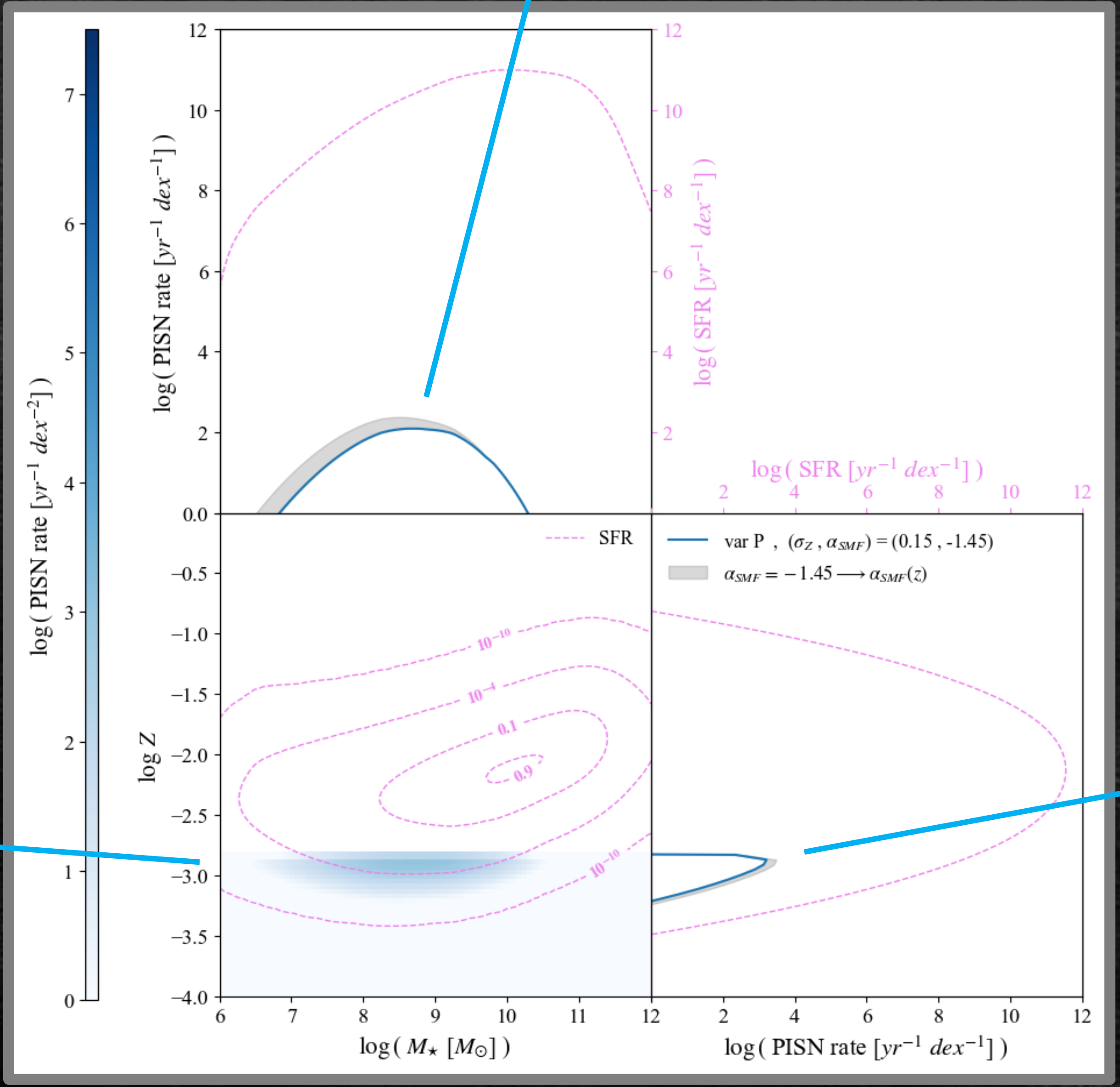

$Z \lesssim Z_{max}$

$Z_{max} = 1.5 \times 10^{-3}$

Host galaxy properties

$M_\star \sim 10^{10} - 10^{11}\ M_\odot$

variation O

$\sigma_Z = 0.35$

$Z_{max} = 1.7 \times 10^{-2}$

$Z_{max} \sim Z^{SFRD}_{peak}$

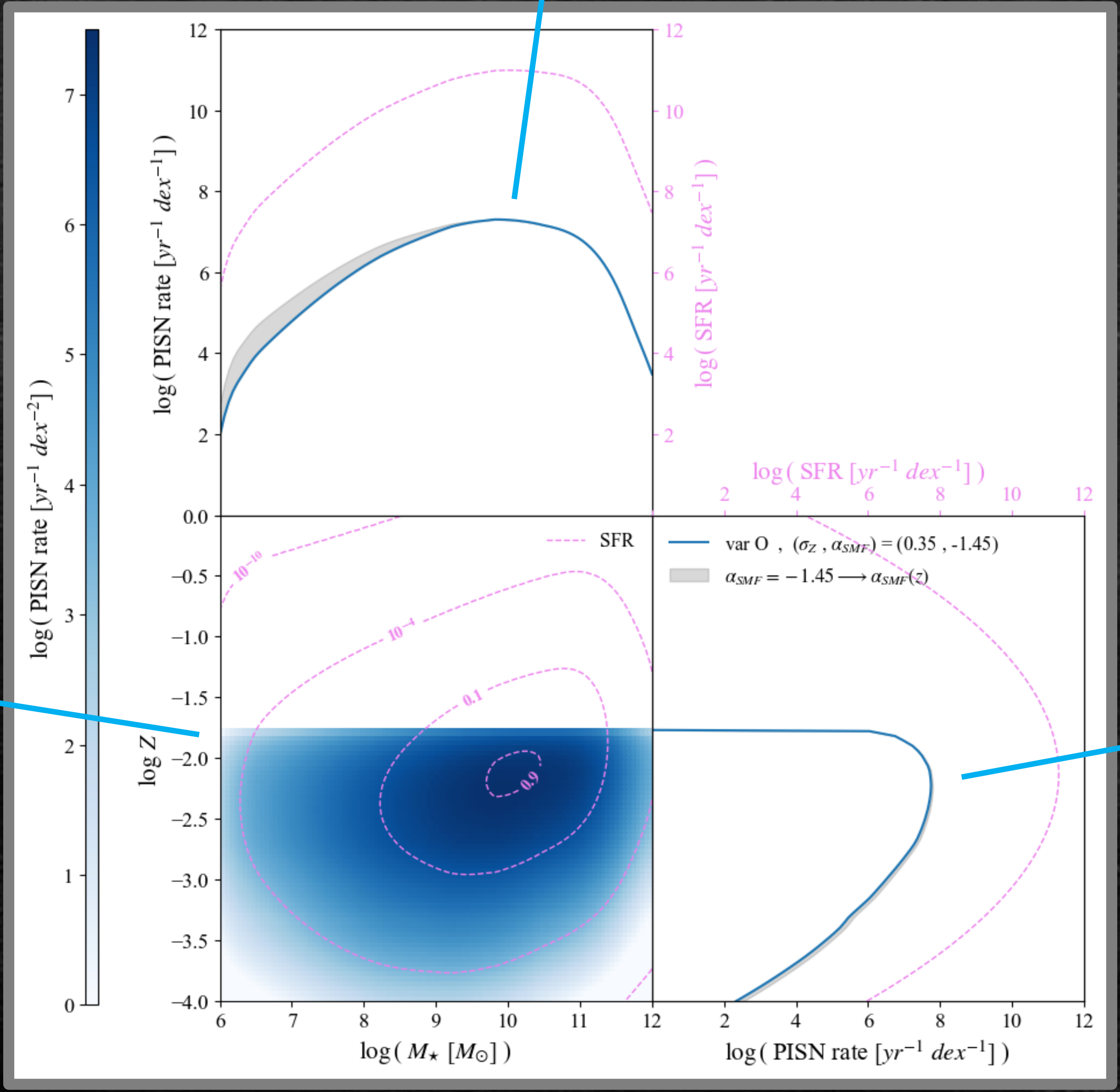

Pop III

peak of PISN rate at
$Z \sim 10^{-2} - 10^{-3}$

→ Pop II stars main PISN progenitors, not Pop III

Pop III SFRD Hartwig et al. 2022

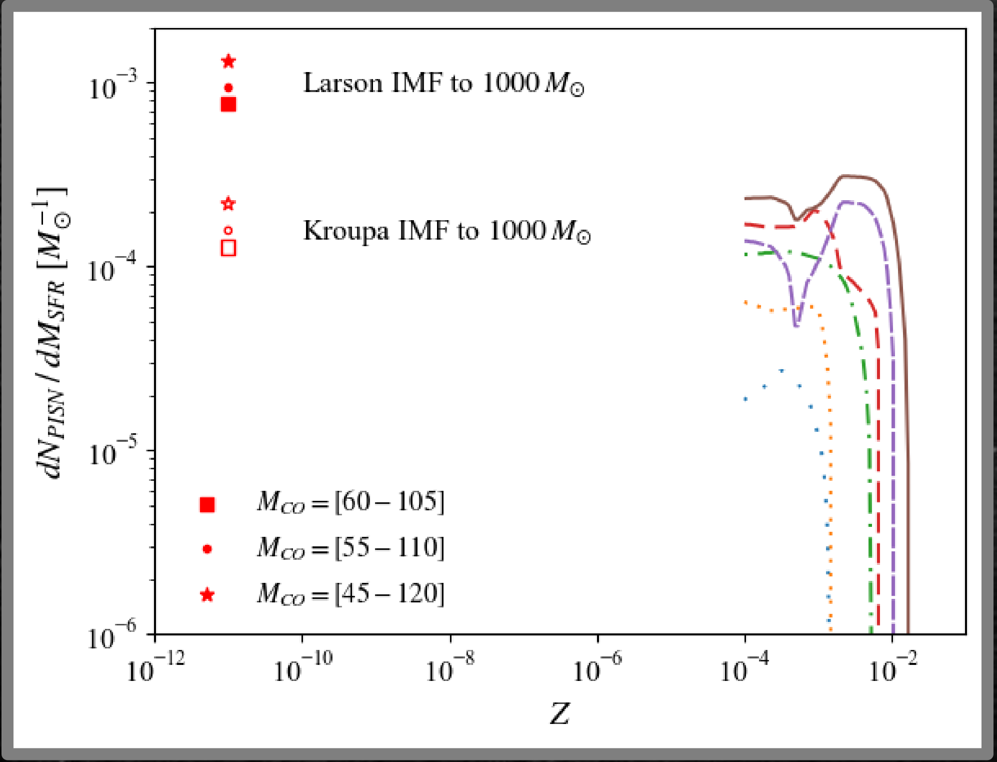

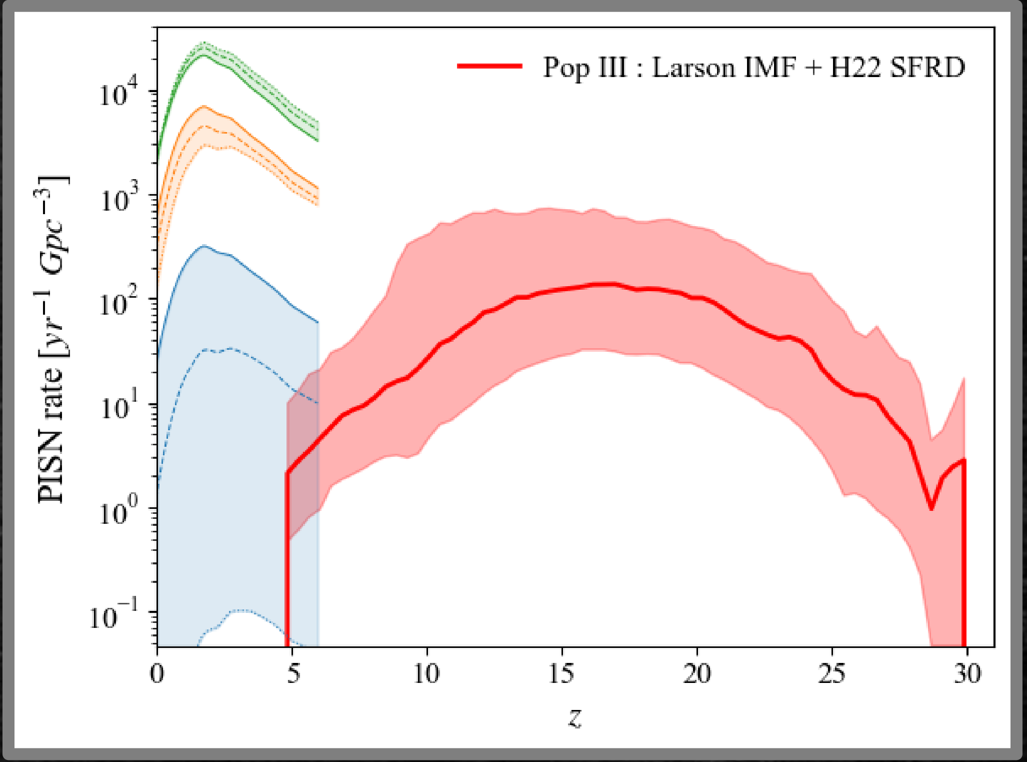

CAVEAT: SFRD and IMF at high z highly uncertain

$$M_{up} = 300\ M_\odot \quad \text{to} \quad 600\ M_\odot$$

$$\frac{dN_{PISN}}{dM_{SFR}}(Z)$$

PISN rate

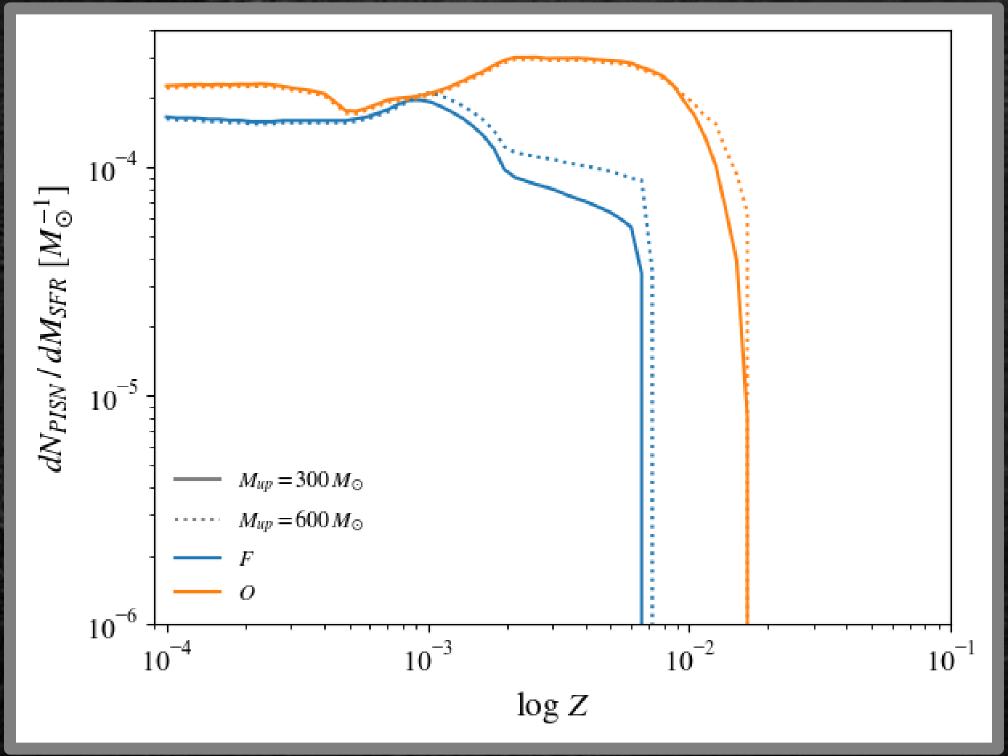

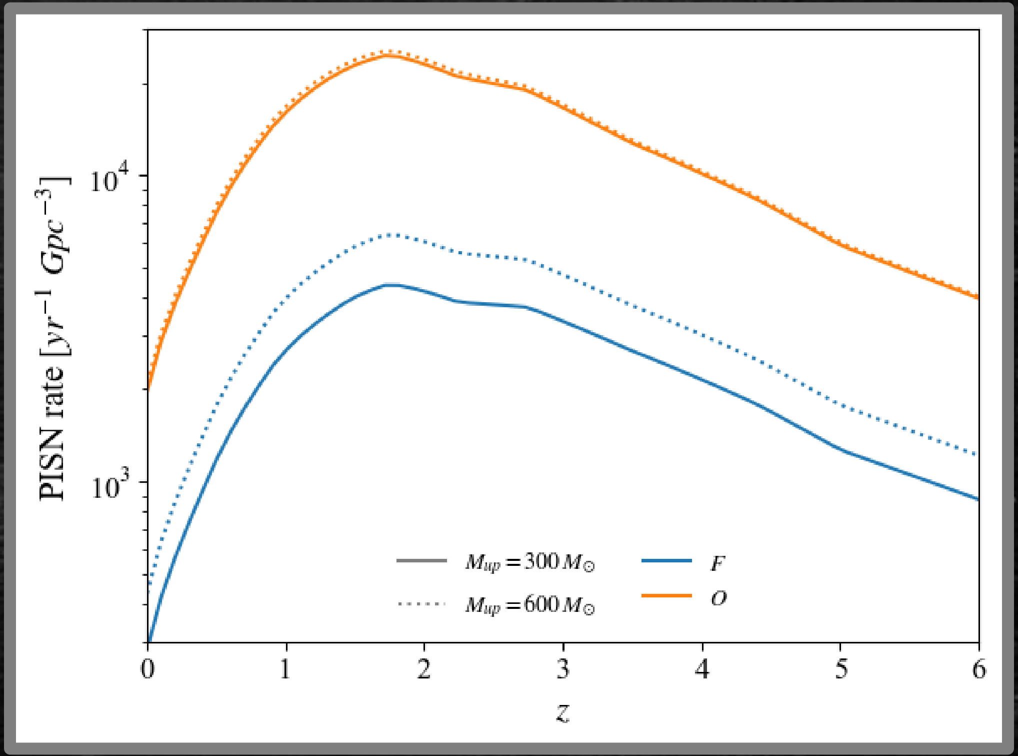

M_{He} criterion

$$\frac{dN_{PISN}}{dM_{SFR}}(Z)$$

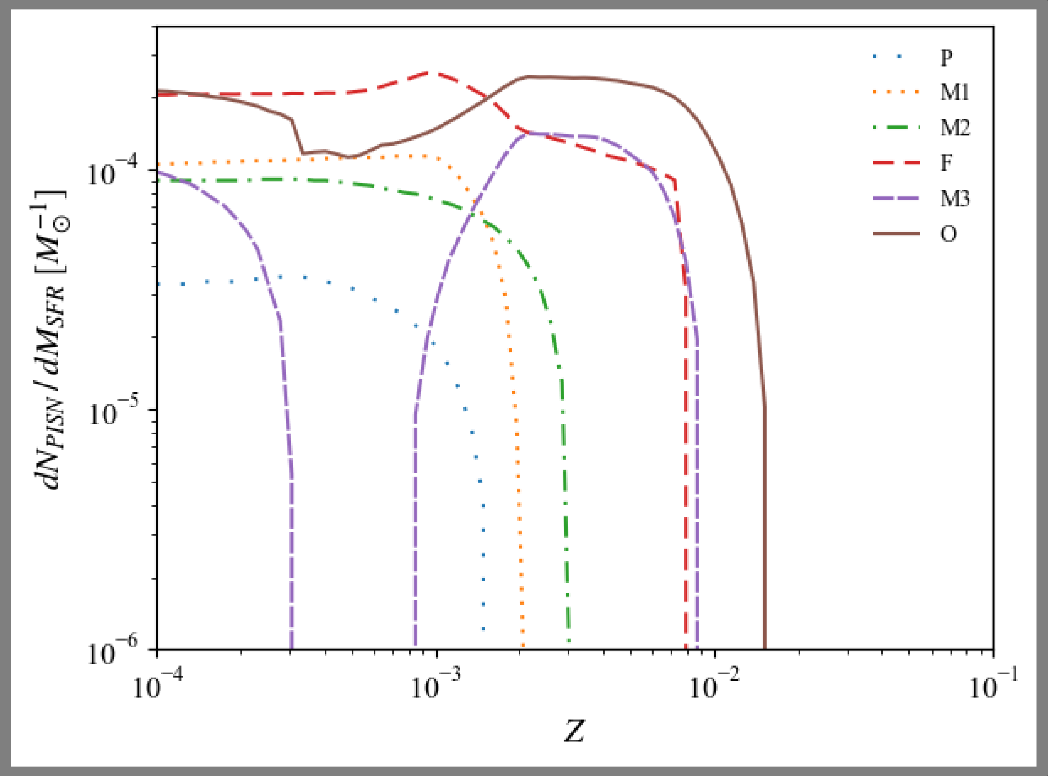

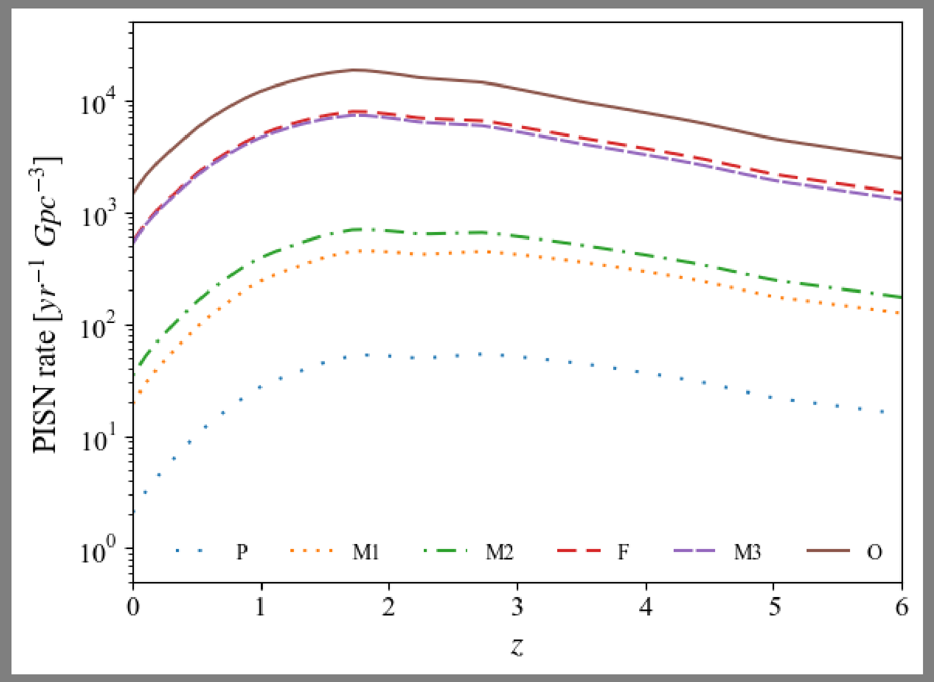

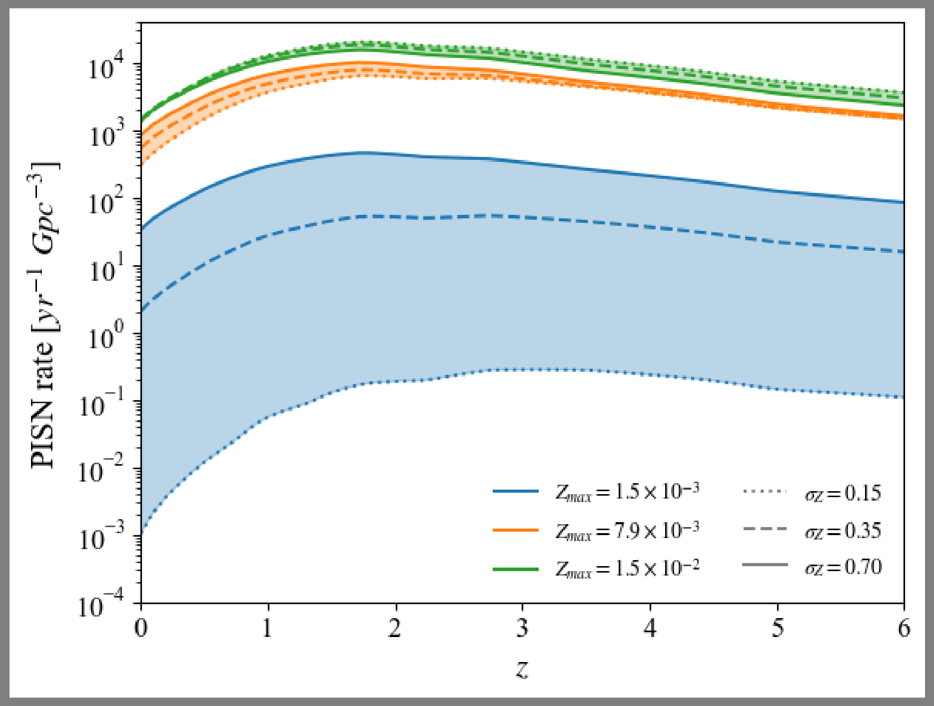

FMR Mannucci et al. 2010

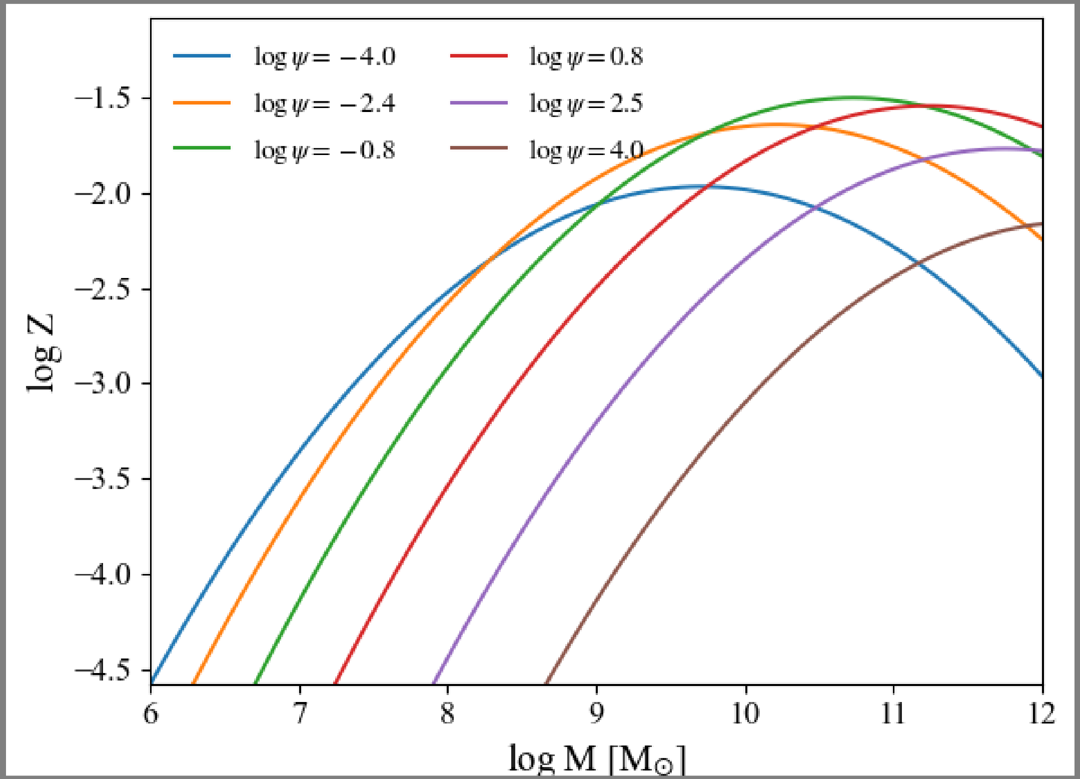

$$12 + log(O/H) = \quad 8.90 + 0.37m - 0.14s - 0.19m^2 + 0.12ms - 0.054s^2$$

$$m = \log(M_\star) - 10$$

$$s = \log(\mathrm{SFR})$$

$$\log Z = 12 + \log(\mathrm{O/H}) - 10.58$$

FMR Mannucci et al. 2010

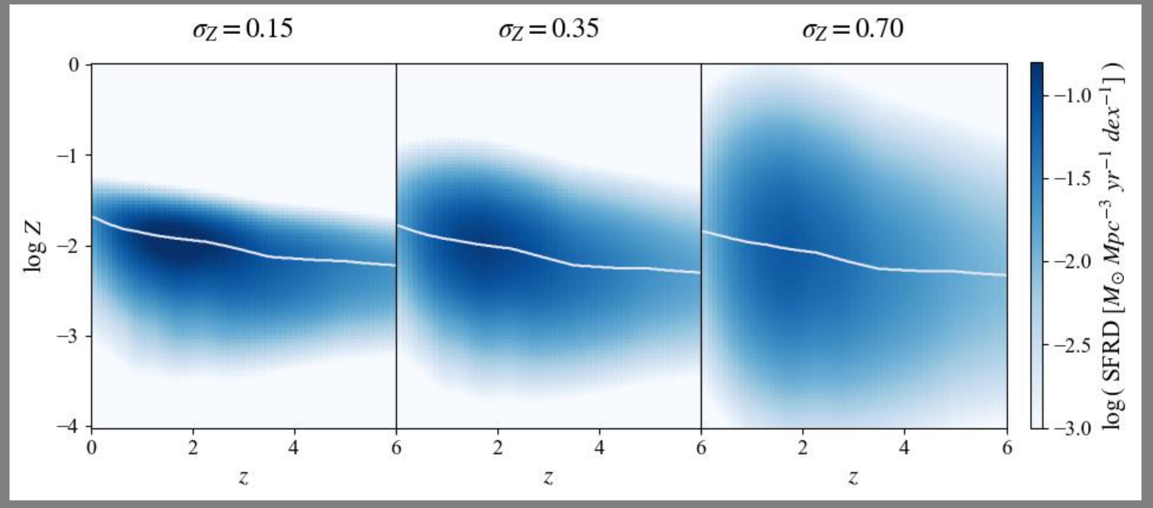

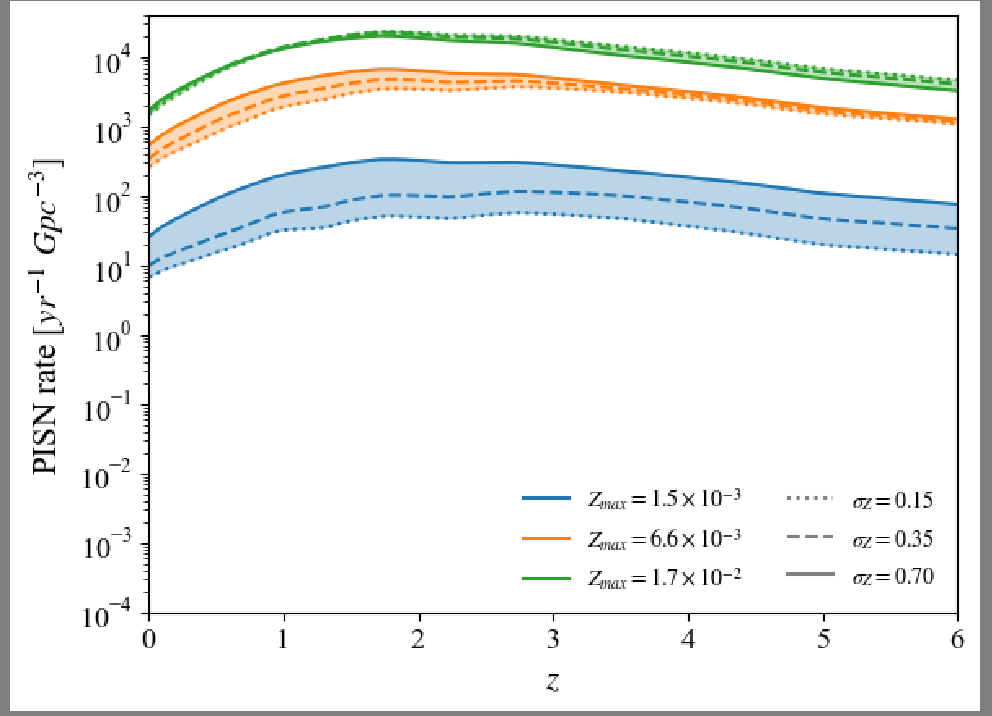

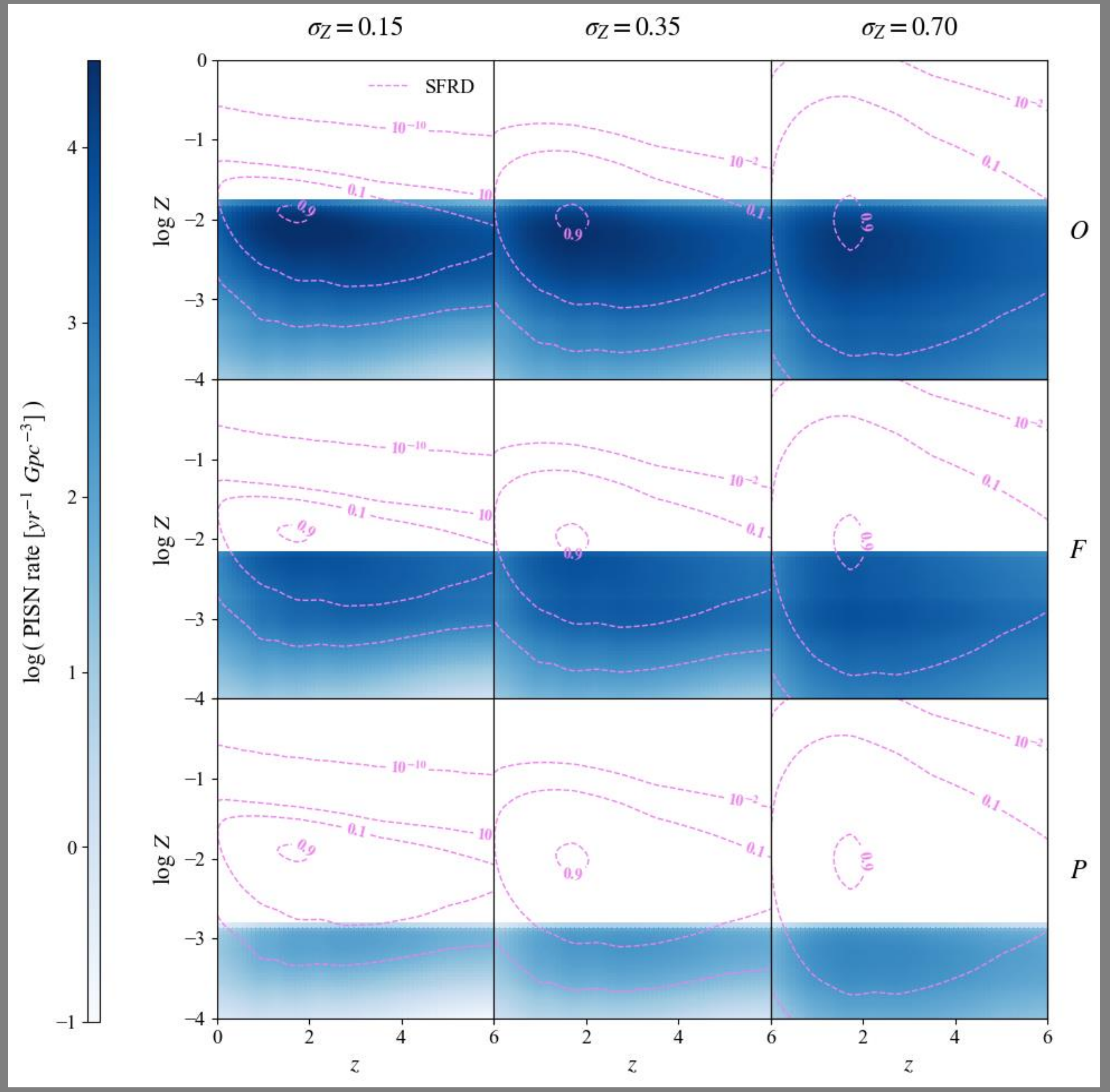

FMR Mannucci et al. 2011

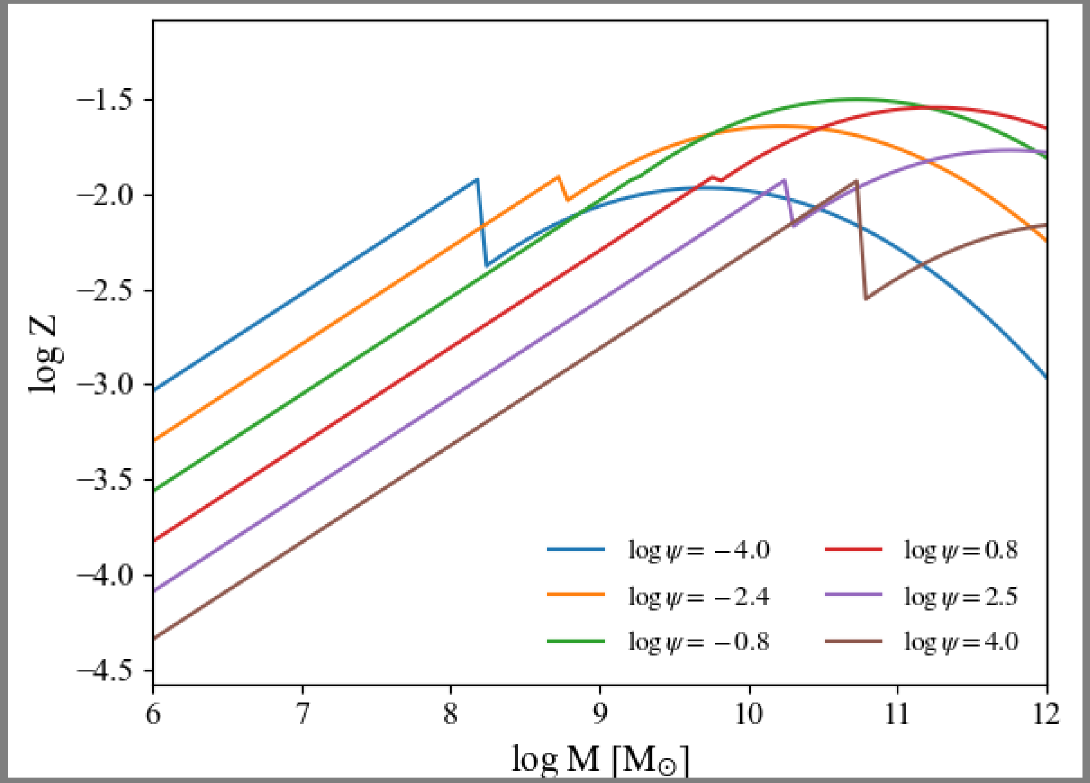

$$12 + \log(\mathrm{O/H}) = 8.90 + 0.37m - 0.14s - 0.19m^2 + 0.12ms - 0.054s^2 \quad \text{for } \mu_{0.32} \geq 9.5$$
$$= 8.93 + 0.51(\mu_{0.32} - 10) \text{ for } \mu_{0.32} < 9.5,$$

$$\mu_\alpha = \log(M_*) - \alpha \log(\mathrm{SFR})$$

$$m = \log(M_\star) - 10$$

$$s = \log(\mathrm{SFR})$$

isolated stellar/binary evolution

Manuel Arca Sedda, Lavinia Paiella,
Cristiano Ugolini, Benedetta Mestichelli

PISNe in dense star clusters

SEVN + hardening

(Iorio et al. 2023)

FASTCLUSTER

(Mapelli et al. 2021)

dependence of PISN production efficiency on cluster properties

STARC

Manuel Arca Sedda